Estrogen re-enhanced prenatal stress-related visceral sensitization and pain regulation

Jinghong Chen (cjhsmch@163.com)
Shanghai Mental Health Center https://orcid.org/0000-0002-7428-9359
Ying Sun
Shanghai Mental Health Center
Jinbao Wei
Shanghai Mental Health Center
Peijun Ju
Shanghai Mental Health Center
Qinjie Li
Division of Gastroenterology, Department of Internal Medicine
John H. Winston
Enteric Neoromuscular Disorders and Visceral Pain Center

Research article

Keywords: chronic prenatal stress, estrogen, visceral pain, neuronal sensitization, excitability, Letrozole

Posted Date: November 9th, 2020

DOI: https://doi.org/10.21203/rs.3.rs-100064/v1

Abstract

Background: Visceral pain is one of the most common sign of irritable bowel syndrome (IBS). Chronic stress during pregnancy may increase visceral pain sensitivity of offspring in a sexdependent way. Combining adult stress in offspring will increase this sensitivity. Based on the evidence implicating estrogen exacerbates visceral hypersensitivity in female rodents in pre-clinical models, we predicted that chronic prenatal stress (CPS) plus chronic adult stress (CAS) will maximize visceral pain sensitivity; and estrogen plays an important role in this hyperalgesia.

Methods: The CPS plus CAS rodent model was established in which the balloon was used to distend colorectum. Meanwhile, the single fiber recording in vivo and patch-clamp experiments in vitro were used to monitor neuronal activity. The RT-PCR, Western Blot, and Immunofluorescence were used to study the effects of CPS and CAS on colon primary afferent sensitivity and molecular or transmission changes. We use Ovariectomy and Letrozole to treate female rats respectively in order to assess the role of estrogen in female-specific enhanced primary afferent sensitization. Letrozole mainly used to reduce estrogen levels.

Results: As predicted, CPS significantly increased single unit afferent fiber activity in L6-S2 dorsal roots in response. Activity was further enhanced by CAS. And the activity in offspring females was significantly greater than the males. Besides, the excitability of colon-projecting dorsal root ganglion (DRG) neurons increases in CPS + CAS rats that was associated with a decrease in transient A-type K+ current. Letrozole treatment decreases the colon DRG neuron excitability in females by decreasing the estrogen levels.

Conclusions: This study adds to the growing evidence for the development of chronic stress induced visceral hypersensitivity in female, which involves estrogen-dependent sensitization of primary afferent colon neurons. Understanding this neurophysiological mechanisms will spur the development of female pain specific therapies.

Background

Visceral pain of colonic origin is the most prominent symptom in irritable bowel syndrome (IBS) patients [1]. Female IBS patients report more severe pain that occurs more frequently and with longer episodes than in male patients [1, 2]. The ratio of female to male IBS is about 2:1 among patients seen in medical clinics [3]. Moreover, females show a higher prevalence of IBS co-morbidities such as anxiety and depression [4-6] and are more vulnerable to stress-induced exacerbation of IBS symptoms compared to males [3, 7, 8].

Clinical studies show that early life adverse experiences are risk factors for the development of IBS symptoms, including visceral pain and ongoing chronic stress, especially abdominal pain [9-12]. These factors contribute to the development of visceral hypersensitivity, a key component of the IBS symptom complex and one that may be responsible for symptoms of pain [13, 14]. Our previous research found that the female offspring of mothers subjected to chronic prenatal stress (CPS) show a markedly greater visceral sensitivity than their male littermates following challenge by another chronic adult stress (CAS)

protocol. A critical molecular event in the development of this female-enhanced visceral hypersensitivity is up-regulation of brain-derived neurotrophic factor (BDNF) expression in the lumbar-sacral spinal cord of female CPS + CAS rats [15]. However, the neurophysiological changes underlying this enhanced female-specific visceral hypersensitivity and the role of hormone in the development of stress-induced visceral hypersensitivity are not well understood.

Visceral hypersensitivity in IBS involves abnormal changes in neurophysiology throughout the brain-gut axis. In IBS, there is evidence for sensitization of primary afferents to jejunal distention and electrical stimulation [16], and there is evidence for increased sensitivity of lumbar splanchnic afferents [17, 18]. In animal models of either early life adverse events [19] or adult stress induced visceral hypersensitivity [20], there is evidence of colon primary afferent sensitization. However, these studies are performed in male rodents. Therefore, in this study, we established a CPS and CAS rodent model to analyse the impact on female colon afferent neuron function and the role of estrogen. Our hypothesis is that female CPS offspring subjected to chronic stress as adults exhibit greater colonic DRG neuron sensitization compared to their male littermates and that this female enhanced visceral sensitization and primary afferent sensitization are estrogen dependent.

Methods

Animals

Experiments were performed on pregnant Sprague-Dawley rats and their 8-16 week old male and female offspring.

CPS and CAS models

Pregnant dams were subjected to a CPS protocol that consisted of a random sequence of twice-daily applications of one of three stress sessions, one hour water avoidance stress, 45 min cold restraint stress or 20 min forced swim stress starting on 6th day and continuing until delivery (21st day). Male and female offspring from the stressed dams were designated CPS rats. Control dams received sham stress and their offspring were designated control rats. As adults (8-16 wks), control and prenatally stressed offspring were challenged by the same CAS protocol for nine days. Ovariectomy (OVX) or sham surgery was performed on female prenatal stress offspring in the 56th day. Daily Letrozole treatment was initiated on the 49th day, 2 weeks prior to initiation of adult stress. Treatment was continued through the stress protocol. Detail schematic diagram is present in **Fig. 1A**.

Rattreatment

Before the treatment of OVX or Letrozole, Vaginal smear test was used to identify the estrus cycle phases of female rats. The OVX or sham surgery was performed on female prenatal stress offspring in the 56th day. The aromatase inhibitor Letrozole (4,4'-(1H-1,2,4-triazol-l-yl-methylene)-bis-benzonitrile; 1.0 mg/kg, oral administration; Novartis) was used in experiment group; and Vehicle (hydroxypropyl cellulose 0.3% in

water) was used in contral group once daily for 14 days. Direct transcutaneous intrathecal injections (i.t.) of estrogen and letrozole were performed respectively as described by Mestre et al. [21]

In vivo single fiber recording of L6-S2 DRG rootlets

Multiunit afferent discharges were recorded from the distal ends of L6-S2 dorsal rootlets decentralized close to their entry into the spinal cord. A bundle of multiunit fibers was distinguished into 2-6 single units off-line using wave mark template matching in Spike 2 software that differentiates spikes by shape and amplitude. Colonic afferent fibers were identified by their response to graded colorectal distention (CRD). Isoflurane, 2.5%, followed by 50 mg/kg, i.p. sodium pentobarbital induced general anesthesia that was maintained by infusing a mixture of pentobarbital sodium + pancuronium bromide + saline by intravenous infusion through the tail vein. Adequacy of anesthesia was confirmed by the absence of corneal and pupillary reflexes and stability of end-tidal CO_2 level. A tracheotomy tube connected to a ventilator system provided a mixture of room air and oxygen. Expired CO_2 was monitored and maintained at 3.5%. Body temperature was monitored and maintained at 37 °C by a servo-controlled heating blanket. A laminectomy from T12 to S2 exposed the spinal cord. The head was stabilized in a stereotaxic frame. The dura was gently opened and a warm mineral oil pool, contained by skin flaps, covered the exposed spinal cord and roots as described previously [22].

Invitropatch clamp recordings in colonic DRG neurons

Retrograde fluorescence label injections

Labeling of colon projecting DRG neurons was performed as previously described [20]. Under general 2% isoflurane anesthesia, the lipid soluble fluorescence dye,1,1’-dioleyl-3,3,3’,3’-tetramethylindocarbocyanine methane-sulfonate (9-DiI, Invitrogen, Carlsbad, CA) (50 mg/mL) was injected into muscularis externae on the exposed distal colon in 8 to 10 sites (2 μL each site). To prevent leakage, the needle was kept in place for 1 min following each injection.

Dissociation and culture of DRG neurons

Rats were deeply anesthetized with isoflurane followed by decapitation. Lumbosacral (L6–S2) DRGs were collected in ice-cold and oxygenated dissecting solution, containing (in mM): 130 NaCl, 5 KCl, 2 KH_2PO_4, 1.5 $CaCl_2$, 6 $MgSO_4$, 10 glucose, and 10 HEPES, pH 7.2 (305 mOsm) [23]. After removal of the connective tissue, the ganglia were transferred to a 5 ml dissecting solution containing collagenase D (1.8 mg/mL; Roche) and trypsin (1.0 mg/mL; Sigma, St Louis, MO), and incubated for 1.5 hours at 34.5°C. DRGs were then taken from the enzyme solution, washed, and put in 0.5 to 2 mL of the dissecting solution containing DNase (0.5 mg/mL; Sigma). Cells were subsequently dissociated by gentle trituration for 10–15 times with fire-polished glass pipettes and placed on acid-cleaned glass coverslips. The dissociated DRG neurons were kept in 1 mL DMEM (with 10% FBS) in an incubator (95% O_2/5% CO_2) at 37°C overnight.

Whole-cell patch clamp recordings from dissociated DRG neurons

Before each experiment, the glass coverslip with DRG neurons was transferred to recording chamber perfused (1.5 mL/min) with external solution containing (10 mM): 130 NaCl, 5 KCl, 2 KH_2PO_4, 2.5 $CaCl_2$, 1 $MgCl_2$, 10 HEPES, and 10 glucose, pH adjusted to 7.4 with NaOH (300 mOsm) at room temperature. Recording pipettes, pulled from borosilicate glass tubing, with resistance of 1–5 MΩ, were filled with solution containing (in mM): 100 $KMeSO_3$, 40 KCl, and 10 HEPES, pH 7.25 adjusted with KOH (290 mOsm). DiI labeled neurons were identified under fluorescent microscope. Whole-cell currents and voltage were recorded from DiI-labeled neurons using Dagan 3911 patch clamp amplifier. Data were acquired and analyzed by pCLAMP 9.2 (Molecular Devices, Sunnyvale, CA). The currents were filtered at 2–5 kHz and sampled at 50 or 100s per point. While still under voltage clamp, the Clampex Membrane Test program (Molecular Devices) was used to determine membrane capacitance, Cm and membrane resistance, Rm, during a 10 ms, 5 mV depolarizing pulse form a holding potential of -60 mV. The configuration was then switched to current clamp (0 pA) for determining other electrophysiological properties. After stabilizing for 2–3 min, resting membrane potential was measured. The minimum acceptable resting membrane potential was -40 mV. Spontaneous activity (SA) was then recorded over two 30 second periods separated by 60 s without recording as described by Bedi and Chen [24].

Transient A-type K^+ current (I_A) recording method in Patch studies

To record voltage-gated K^+ current (Kv), Na^+ in control external solution was replaced with equimolar choline and the Ca^{2+} concentration was reduced to 0.03 mM to suppress Ca^{2+} currents and to prevent Ca^{2+} channels becoming Na^+ conducting. The reduced external Ca^{2+} would also be expected to suppress Ca^{2+}-activated K^+ current. The current traces of Kv in DRG neurons were measured at different holding potentials. The membrane potential was held at -100 mV and voltage steps were from -40 to +30 mV to record the total Kv. The membrane potential was held at -50 mV to record the sustained Kv. The I_A currents were calculated by subtracting the sustained current from the total current. The current density (in pA/pF) was calculated by dividing the current amplitude by cell membrane capacitance.

Real time RT-PCR

Total RNA was extracted using the RNeasy Mini Kit (QIAGEN, Valencia, CA). One microgram of total RNA was reverse-transcribed using SuperScript™ III First-Strand Synthesis System. PCR was performed on a StepOnePlus thermal cycler with 18S as the normalizer using Applied Biosystems primer/probe set Rn02531967_s1 directed against the translated exon IX. Fold-change relative to control was calculated using the ΔΔCt method (Applied Biosystems).

Western Blot

Samples were lysed in RIPA buffer containing protease inhibitor cocktail and phenylmethanesulfonyl fluoride. Lysates were incubated for 30 min on ice and then centrifuged at 10 000×g for 10 min at 4 °C.

The protein concentration in the supernatant was determined using BCA kits with bovine serum albumin as a standard. Equal amounts of protein (30 µg per lane) were separated with 10% SDS-PAGE and then transferred to nitrocellullose membranes (Bio-Rad, USA). The membrane was blocked in Li-Cor blocking buffer for 1 h at room temperature and then incubated with primary antibodies. BDNF antibody (Santa Cruz Biotechnologies, Santa Cruz, CA) was used at 1:200 dilution; Nerve growth factor (NGF) antibody (Abcam, MA) was used at 1:1000 dilution; β-actin antibody (Sigma Aldrich, St Louis) was used at 1:5000 dilution. Secondary antibodies used were donkey anti-rabbit alexa fluor 680 (Invitrogen) and goat anti-mouse IRDye 800 (Rockland). Images were acquired and band intensities measured using the Li-Cor Odyssey system (Li-Cor, Lincoln, Nebraska).

Immunofluorescence

Frozen sections of colon mounted on glass slides from control, CAS, CPS and CPS + CAS female rats were rehydrated in phosphate buffered saline at room temperature. All slides were treated for antigen retrieval and blocked with 10% normal goat serum (diluting in 0.3% phosphate buffered saline-Triton) for 1 h. Primary antibody NGF in antibody diluent (Renoir Red, Biocare Medical, Concord, CA) were incubated at 4^{o}C overnight. The slides were exposed to fluorescent dye conjugated secondary antibody for 2 h at room temperature. Slides were counterstained with DAPI and coverslipped. Images were taken in fluorescence mode on an Olympus laser scanning confocal microscope and the average signal intensity was calculated by the bundled software.

Serum Estradiol and norepinephrine Levels

Serum estradiol, adrenocorticotropic hormone (ACTH), and norepinephrine levels were measured using specific ELISA kits for each analyte (CSB-E05110r, CSB-E06875r, CSB-E07022, Cusabio Bioteck CO.LTD, USA) according to the manufacturer's instructions.

Data analyses

Single fiber responses (impulses/second) to CRD were calculated by subtracting SA from the mean of 30 seconds of the maximal activity during distension. Fibers were considered responsive when CRD increased their activity 30% greater than the baseline value. Mechanosensitive single units were classified into high-threshold (>20 mmHg) and low-threshold (≤20 mmHg) on the basis of their response threshold and profile during CRDs. Single fiber activity data were analyzed using ANOVA with repeated measures; CRD intensity was the repeated factor and experimental group as the between group factor. If significant main effects were present, the individual means were compared using the Fisher post-hoc test.

Results

Effects of CPS plus CAS on primary afferent responses to CRD in male and female rats

The basal activity of a spinal afferent fiber was defined as the average number of action potentials per second (impulses/sec) in the 60 second period before the onset of a distention stimulus. 66% of the afferent fibers under study displayed SA in male controls. In the female controls, SA was significantly greater than control males, 0.71 ± 0.21 vs 1.24 ± 0.20 imp/sec (Fig. 1B). The average single fiber activity in response to CRD was significantly higher in female control rats compare to male controls (Fig. 1C). We found that the enhanced sensitization in female rats mainly came from the low threshold fibers (Fig. 1D, E).

To assess the effects of CPS + CAS on colon afferent fiber activities, we compared average single colon afferent fiber activities projecting from dorsal roots S1-L6 in response to CRD in male and female control, CPS, control + CAS and CPS + CAS rats recorded approximately 24 hours after the last stressor. Within females, CPS significantly increased single unit afferent activities in response to CRD vs control female rats (Fig. 1F). CAS alone enhanced single unit activities compared to control. The average afferent responses after CAS in female prenatally stressed rats were significantly greater (44.0% increase rate compare to female control and 39.3% increase rate compare to CAS only female rats). Within males, CPS had no significant effect on primary afferent responses (Fig. 1G). When we compared males to females within each experimental group, we found that average single fiber activities were significantly higher in female compared to male CPS + CAS rats (Fig. 1F, G). This greater activity may contribute to the enhanced female visceral hypersensitivity previously reported in this model. Average single fiber activity of control, CPS and CAS females were significantly greater than their respective male experimental groups (Fig. 1F, G). Both CAS and CPS + CAS significantly increased primary afferent responses compared to control and to CPS. Thus, our CPS and CAS protocols generally produce sensitization of colon projecting primary afferent fibers with greatest effects produced by the combination of CPS + CAS in both males and females.

Increase in Excitability of Colon-projecting Lumbosacral DRG Neurons from female CPS + CAS rats

To elucidate the electrophysiological basis for enhanced stress-induced primary afferent activity in female rats, we performed patch clamp studies on acutely dissociated retrograde labelled colon projecting neurons from the L6-S2 DRG from control, prenatal stress, adult stress only and CPS + CAS female rats isolated 24 hours after the last adult stressor (Fig. 2A). Input resistance (Fig. 2C) and rheobase (Fig. 2D) were significantly decreased in neurons from CPS + CAS rats compared to the other three groups. The number of action potentials elicited at either 2X or 3X the rheobase were significantly greater in adult stress and CPS + CAS neurons compared to control and to CPS neurons (Fig. 2B, E). CAS significantly increased action potential overshoot with or without CPS (Fig. 2F), but it did not significantly alter the other electrophysiological characteristics, such as spontaneous spike number, membrane capacitance (pF), resting membrane potential, cell diameter, time constant, action potential amplitude, and duration of DRG neurons (Table 1).

Table 1
Electrophysiological characteristics properties of dorsal horn neurons

Classification	Ctr. (n = 36)	CAS (n = 34)	CPS (n = 29)	CAS + CPS (n = 45)
Spontaneous spike number	7.4 ± 4.0	16.9 ± 6.6	11.7 ± 4.8	44.8 ± 14.6; ***
Membrane capacitance (pF)	72.1 ± 4.9	95.4 ± 5.8	85.1 ± 6.2	93.8 ± 8.9; *
Action potential threshold (mV)	-27.1 ± 2.5	-29.2 ± 1.8	-34.6 ± 1.6	− 38.6 ± 1.4; ***
Resting membrane potential (mV)	-60.1 ± 1.7	-50.1 ± 1.3	-53.8 ± 1.5	-56.4 ± 1.3
Cell diameter (μm)	32 ± 0.9	29 ± 0.6	31 ± 0.8	31 ± 0.6
Time constant (um)	545.5 ± 51.1	737.7 ± 70.4	595.9 ± 54.1	535.3 ± 42.5
Action potential amplitude (mV)	79.0 ± 4.7	80.2 ± 3.9	77.4 ± 4.2	85.6 ± 3.7
Duration (ms)	8.38 ± 0.97	11.2 ± 0.95	12.3 ± 1.83	8.89 ± 0.60

The value equal means ± SE. Statistical significance is indicated by *($P < 0.05$), **($P < 0.01$) and ***($P < 0.001$) compared with the control group. n = number of observations.

There were a significantly greater percentage of neurons displaying SA in CPS + CAS rats vs. control or CPS only rats (Fig. 2G). Under voltage-clamp conditions, neurons from female CPS + CAS, CAS, CPS and control groups exhibited I_A and sustained outward rectifier K^+ currents (I_K) (Fig. 2H). Compared with the other three groups, DRG neurons from CPS + CAS rats demonstrated a significantly reduced average I_A ($p < 0.05$) (Fig. 2H). However, the average I_K density although decreased was not altered significantly.

Effects of CPS and/or CAS on plasma estrogen concentrations

We did the vaginal smear test to identify the estrus cycle phases by identifying the Vaginal Cytological cell types. Estrogen concentration was significantly higher in CPS proestrus/estrus phase compared to control diestrus, control proestrus/estrus and CPS diestrus porestrus ($p < 0.05$; Fig. 3A). Comparison of the plasma estrogen concentrations in control, CAS, CPS, CPS + CAS showed that CPS significantly increased plasma estrogen levels compared to the control rats and that CAS increased plasma estrogen level compared to the control and CPS rats (Fig. 3B).

To determine whether estrogen contributed to stress-induced visceral hypersensitivity in prenatal stressed females, we reduced plasma estrogen levels with either OVX or Letrozole treatment. OVX significantly lowered serum estradiol levels before and after CAS (Fig. 3C). Treatment was continued throughout CAS. After treatment with Letrozole, serum estradiol levels were significantly reduced (Fig. 3D). To study the effects of gender and stress on norepinephrine and ACTH levels, we measured plasma norepinephrine levels in female rats from all four experimental groups. CAS alone significantly increased plasma norepinephrine levels compared to control and to CPS alone (Fig. 3E) Plasma norepinephrine levels were

significantly increased in CPS + CAS rats compared to CAS alone as well as to control and CPS. Plasma ACTH levels were significantly increased in CPS + CAS rats compared to control. (Fig. 3F).

Effects of Letrozole treatment on colon DRG neuron excitability

We performed patch clamp experiments on acutely isolated retrograde labelled DRG neurons from CPS + CAS females with or without letrozole treatment 24 hours after the last adult stressor. Letrozole treatment significantly increased rheobase (Fig. 4A), and significantly reduced input resistance (Fig. 4B). Action potential overshoot (Fig. 4C) and the number of action potentials elicited by a current injection at either 2X or 3X rheobase were significantly reduced by letrozole treatment (Fig. 4D). Other electrophysiological properties were not significantly altered (Table 2). We also recorded Electromyographic activity to determine whether the reduction in visceral sensitivity in female CPS + CAS rats caused by OVX or systemic Letrozole treatment can reduced visceromotor response. We found that the Electromyographic of CRD was significantly reduced in OVX rats after 24 hours after the last adult stressor (**Supplementary Fig. 1A**) or in systemic Letrozole treated rats compared to vehicle both before and after CAS (**Supplementary Fig. 1B**). These findings demonstrated a significant decrease in excitability of colon projecting L6-S2 neurons.

Table 2
Electrophysiological characteristics properties of dorsal horn neurons after letrozole treatment

Classification	**Veh.+CAS + CPS (n = 60)**	**Let + CAS + CPS (n = 27)**
Spontaneous spike number	34.6 ± 11.3	8.04 ± 4.62; ***
Membrane capacitance (pF)	86.8 ± 7.1	83.7 ± 6.7
Action potential threshold (mV)	-34.6 ± 1.6	− 27.6 ± 2.1; *
Resting membrane potential (mV)	-54.9 ± 1.3	-54.6 ± 2.2
Cell diameter (μm)	31 ± 0.5	27 ± 1.6
Time constant (um)	502.7 ± 34.5	454.0 ± 36.6
Action potential amplitude (mV)	90.9 ± 3.7	89.8 ± 7.2
Duration (ms)	8.67 ± 0.63	10.70 ± 2.22
The value equal means ± SE. Statistical significance is indicated by *($P < 0.05$), **($P < 0.01$) and ***($P < 0.001$) compared with the control group. n = number of observations.		

Spinal cord BDNF levels regulated by estrogen

To investigate the effect of estrogen on BDNF expression, we measured BDNF mRNA and protein levels in lumbar sacral spinal cord of OVX and Sham CPS + CAS female rats. Systemic estradiol administration to naïve cycling females produced significant increases in plasma estrogen (Fig. 5A), lumbar sacral spinal

cord BDNF mRNA (Fig. 5B) and protein (Fig. 5C). We also measured BDNF mRNA and protein levels in lumbar sacral spinal cord of OVX and Sham CPS + CAS female rats. BDNF mRNA and protein expression were significantly suppressed by OVX compared to Sham rats (**Supplementary Fig. 1C**). Another experiment showed that intrathecal infusion of estrogen into naïve female rats significantly increased BNDF protein levels, which proved that estrogen can reverse the experimental results and contribute to the response to visceral pain (**Supplementary Fig. 1D**).

Peripheral NGF level increased in CPS + CAS female rats

We examined NGF expression in the colon in females from all four experimental groups by immunohistochemistry (Fig. 6A). Morphometric analysis showed that CAS and CPS + CAS significantly increased NGF levels in the colon wall with the increase in CPS + CAS significantly greater that of CAS alone (Fig. 6B). Western blotting showed that NGF protein was significantly up-regulated in CPS + CAS compared to controls (Fig. 6C).

Discussion

Our enhanced chronic stress-induced visceral hypersensitivity in female prenatally rats is associated with an increase in the responses of lumbosacral nerve fibers to CRD in both male and female rats. These findings are further supported by our data showing increased excitability of colon projecting DRG neurons from females in patch clamp studies. The magnitude of this sensitization is greatest in female CPS + CAS rats suggesting that this sensitization makes a major contribution to the observed enhanced female visceral hypersensitivity in our model. We focused on lumbar sacral afferent fibers and dissociated neurons in patch clamp studies. It is possible TL neurons also contribute (CAS in males sensitizes TL neurons).

Chronic stress is known to increase the excitability of colon projecting DRG neurons in rats and mice. In adult male Sprague Dawley rats, colon DRG neuron sensitization was driven by increases in NGF expression in the colon muscularis externa [20]. In our model we observe a significant increase in colon NGF, but its potential role in primary afferent sensitization and visceral hypersensitivity was not investigated in this study. Other studies in male mice show that stress in the form of water avoidance stress significantly increases excitability of colon projecting DRG neurons and that stress mediators corticosterone and norepinephrine working together can increase DRG neuron excitability in vitro [25, 26]. Neonatal maternal deprivation sensitizes colon projecting neurons in adult males [27]. In our study, we find significant increases in serum levels of norepinephrine in CPS + CAS females. However, daily systemic treatment with adrenergic antagonists during the adult stress protocol failed to reduce visceral hypersensitivity in female newnatal + adult stress rats [20] suggesting that norepinephrine did not play a major role in the acquisition of enhanced female visceral hypersensitivity or primary afferent sensitization in our model.

We find significant decreases in the transient potassium I_A current in neurons isolated from CPS + CAS females compared to the other three experimental groups. Declines in A type Kv currents in DRG neurons are associated with persistent pain in multiple chronic pain models [28]. Whether this decline is caused by changes in channel properties or expression was not investigated in this study. However, another study demonstrates that estrogen significantly shifted the activation curve for I_A current in the hyperpolarizing direction and that estrogen inhibited Kv (+) channels in mouse DRG neurons through a membrane ER-activated non-genomic pathway [29].

Our results show that excitability of colon projecting neurons in CPS + CAS females is significantly reduced by systemic letrozole treatment suggesting that estrogen contributes to this sensitization process. Previous studies show that estrogen receptors expressed on primary afferent neurons contribute to enhanced sensitivity in various pain models [30–33]. One study finds no decline in the responses of colon projecting nerve fibers to CRD following OVX and finds no detectable estrogen receptor alpha immunoreactivity in colon projecting DRG neurons [34]. The reasons for these differing results are not clear although local production of estrogen in DRG neurons could be sufficient to sustain sensitization.

NGF and its receptors play important roles in the mechanism of visceral pain and hyperalgesia in woman. For example, the endometriosis is an estrogen-dependent and commonly encountered disease in women. The main symptoms are various types of pelvic pain which have a serious effect on women's physical and mental health, but the mechanisms of pain are still unclear. Recent studies showed that NGF can promote neural cell proliferation and differentiation, induce the expression and release of neuropeptides and increase the number of sensory neurons through binding nerve cell receptor.

Conclusion

In this study, we examine the difference of sex and effects estrogen on the acquisition of enhanced visceral hypersensitivity in femal CPS + CAS rats. Our study shows that estrogens act in the spinal cord and the primary afferent neurons to enhance visceral nociception. Acute blockade of the endogenous synthesis of estrogens in the rat spinal cord may significantly reduce visceral hypersensitivity, suggesting that locally produced estrogen can regulate nociceptive neurons to modulate visceral hypersensitivity. Chronic stress-estrogen-BDNF axis sensitizes visceral hypersensitivity in female offspring subjected to CPS. The development of chronic stress induced visceral hypersensitivity in female rats is estrogen dependent. A key component of this hypersensitivity is estrogen dependent sensitization of primary afferent colon neurons. Our findings provide key scientific evidence in a preclinical model in support of developing gender-based treatment for pain in IBS.

We investigated herein whether estrogen re-enhanced visceral pain sensitivity in chronic prenatal stress (CPS) plus chronic adult stress (CAS) rodent models. After using physical Ovariectomy (OVX) or chemical inhibitor Letrozole treatment to reduce estrogen levels, we find that the visceral hyperalgesia, colonic afferant neuronal excitability, nerve growth factor (NGF), brain-derived neurotrophic factor (BDNF), and Estrogen all were increased. The findings indicate that the chronic stress induced visceral hypersensitivity

is estrogen dependent and the hypersensitivity is estrogen dependent sensitization of primary afferent colon neurons, which provide key scientific evidence in a preclinical model in support of developing gender-based pain management.

Abbreviations

IBS: irritable bowel syndrome; CPS: chronic prenatal stress; CAS: chronic adult stress; DRG: dorsal root ganglion; BDNF: brain-derived neurotrophic factor; OVX: ovariectomy; CRD: colorectal distention; SA: Spontaneous activity; I_A: transient A-type K^+ current; Kv: voltage-gated K^+ current; NGF: nerve growth factor; ACTH: adrenocorticotropic hormone

Declarations

Availability of data and materials

The datasets supporting the conclusions of this article are included within the article and its additional supplementary files.

Acknowledgements

The authors would like to acknowledge the essential intellectual contributions of our recently deceased mentor, Dr. Sushil K. Sarna. His guidance was essential to the successful completion of these studies. Thanks to Usman Ali for assistance in arrangement and submitting the manuscript.

Funding

This work was supported by grants from the NIDDK: 1R01 DK111819-01A1 and 5R01DK03234628. This study was also supported in part by grants from the National Natural Science Foundation of China (#81571326 to JHC).

Authors' contributions

Conceived and designed the experiments: JC and JHW; performed the experiments: JC, YS, JW, PJ, QL and JHW; analyzed the data: JC, YS, JW, PJ, QL and JHW; and preparation of the paper: JC, YS, JW, PJ, QL and JHW.

Ethics declarations

Ethics approval and consent to participate

The Institutional Animal Care and Use Committee of the University of Texas Medical Branch at Galveston, TX approved all animal procedures.

Consent for publication

Not applicable.

Competing interests

None of the authors of this manuscript have any conflicts of interests to report.

References

1. Drossman DA, Camilleri M, Mayer EA, Whitehead WE. AGA technical review on irritable bowel syndrome. Gastroenterology. 2002; 123: 2108-31. https://doi.org/10.1053/gast.2002.37095
2. Taub E, Cuevas JL, Cook EW, Crowell M, Whitehead WE. Irritable bowel syndrome defined by factor analysis. Gender and race comparisons. Dig Dis Sci. 1995; 40: 2647-55. https://doi.org/10.1007/BF02220455
3. Chang L, Heitkemper MM. Gender differences in irritable bowel syndrome. Gastroenterology. 2002; 123: 1686-701. https://doi.org/10.1053/gast.2002.36603
4. Cain KC, Jarrett ME, Burr RL, Rosen S, Hertig VL, Heitkemper MM. Gender differences in gastrointestinal, psychological, and somatic symptoms in irritable bowel syndrome. Dig Dis Sci. 2009; 54:1542-9. https://doi.org/ 10.1007/s10620-008-0516-3
5. Li X, Tian X, Lv L, Hei G, Huang X, Fan X, Zhang J, Zhang J, Pang L, Song X. Microglia activation in the offspring of prenatal Poly I: C exposed rats: a PET imaging and immunohistochemistry study. General Psychiatry. 2018; https://doi.org/10.1136/gpsych-2018-000006
6. Baker A, Simon N, Keshaviah A, Farabaugh A, Deckersbach T, Worthington JJ, Hoge F, Fava M, Pollack MP. Anxiety Symptoms Questionnaire (ASQ): development and validation. General Psychiatry. 2019; 32: 1-11. https://doi.org/10.1136/gpsych-2019-100144
7. Mayer EA, Tillisch K. The brain-gut axis in abdominal pain syndromes. Annu Rev Med. 2011; 62: 381-96. https://doi.org/10.1146/annurev-med-012309-103958
8. Enck P, Aziz Q, Barbara G, Farmer AD, Fukudo S, Mayer EA, Niesler B, Quigley EM, Rajilić-Stojanović M, Schemann M, Schwille-Kiuntke J, Simren M, Zipfel S, Spiller RC. Irritable bowel syndrome. Nature Reviews Disease Primers. 2016; 2: 1-24. https://doi.org/10.1038/nrdp.2016.14
9. Talley NJ, Fett SL, Zinsmeister AR. Self-reported abuse and gastrointestinal disease in outpatients: association with irritable bowel-type symptoms. Am J Gastroenterol. 1995; 90: 366-71.
10. Leserman J, Drossman DA. Relationship of abuse history to functional gastrointestinal disorders and symptoms: some possible mediating mechanisms. Trauma Violence Abuse. 2007; 8: 331-43. https://doi.org/10.1177/1524838007303240
11. Bradford K, Shih W, Videlock EJ, Presson AP, Naliboff BD, Mayer EA, Chang L. Association between early adverse life events and irritable bowel syndrome. Clin Gastroenterol Hepatol. 2012; 10: 385-90. http://doi.org/10.1016/j.cgh.2011.12.018
12. Mou L, Lei W, Chen J. Mediating effect of interpersonal relations on negative emotions and dysmenorrhea in female adolescents. General Psychiatry. 2019; 32:e100008.

https://doi.org/10.1136/gpsych-2018-100008.

13. Farzaei MH, Bahramsoltani R, Abdollahi M, Rahimi R. The Role of Visceral Hypersensitivity in Irritable Bowel Syndrome: Pharmacological Targets and Novel Treatments. J Neurogastroenterol Motil. 2016; 22: 558-74. https://doi.org/10.5056/jnm16001
14. Simrén M, Törnblom H, Palsson OS, van Tilburg MA, Van Oudenhove L, Tack J, Whitehead WE. Visceral hypersensitivity is associated with GI symptom severity in functional GI disorders: consistent findings from five different patient cohorts. Gut. 2017; S82. https://doi.org/10.1136/gutjnl-2016-312361
15. Winston JH, Li Q, Sarna SK. Chronic prenatal stress epigenetically modifies spinal cord BDNF expression to induce sex-specific visceral hypersensitivity in offspring. Neurogastroenterol Motil. 2014; 26: 715-30. https://doi.org/10.1111/nmo.12326
16. Accarino AM, Azpiroz F, Malagelada JR. Selective dysfunction of mechanosensitive intestinal afferents in irritable bowel syndrome. Gastroenterology. 1995; 108: 636-43. https://doi.org/10.1016/0016-5085(95)90434-4
17. Munakata J, Naliboff B, Harraf F, Kodner A, Lembo T, Chang L, Silverman DH, Mayer EA. Repetitive sigmoid stimulation induces rectal hyperalgesia in patients with irritable bowel syndrome. Gastroenterology. 1997; 112: 55-63. https://doi.org/10.1016/S0016-5085(97)70219-1
18. Yang B, Wei J, Ju P, Chen J. Effects of regulating intestinal microbiota on anxiety symptoms: A systematic review. General Psychiatry. 2019; 32: e100056. https://doi.org/doi: 10.1136/gpsych-2019-100056
19. Lin C, Al-Chaer Long-term sensitization of primary afferents in adult rats exposed to neonatal colon pain. Brain Res. 2003; 971: 73-82. https://doi.org/10.1016/S0006-8993(03)02358-8
20. Winston JH, Xu GY, Sarna SK. Adrenergic stimulation mediates visceral hypersensitivity to colorectal distension following heterotypic chronic stress. Gastroenterology. 2010; 138: 294-304. https://doi.org/10.1053/j.gastro.2009.09.054
21. Mestre C, Pélissier T, Fialip J, Wilcox G, Eschalier A. A method to perform direct transcutaneous intrathecal injection in rats. J Pharmacol Toxicol Methods. 1994; 32: 197-200. https://doi.org/10.1016/1056-8719(94)90087-6
22. Chen J, Winston JH, Sarna SK. Neurological and cellular regulation of visceral hypersensitivity induced by chronic stress and colonic inflammation in rats. Neuroscience. 2013; 248: 469-78. https://doi.org/10.1016/j.neuroscience.2013.06.024
23. Xu GY, Shenoy M, Winston JH, Mittal S, Pasricha PJ. P2X receptor-mediated visceral hyperalgesia in a rat model of chronic visceral hypersensitivity. Gut. 2008; 57: 1230-37. https://doi.org/10.1136/gut.2007.134221
24. Bedi SS, Yang Q, Crook RJ, Du J, Wu Z, Fishman HM, Grill RJ, Carlton SM, Walters ET. Chronic spontaneous activity generated in the somata of primary nociceptors is associated with pain-related behavior following spinal cord injury. Journal of Neuroscience the Official Journal of the Society for Neuroscience. 2010; 30: 14870. https://doi.org/10.1523/JNEUROSCI.2428-10.2010

25. Ibeakanma C, Ochoa-Cortes F, Miranda-Morales M, McDonald T, Spreadbury I, Cenac N, Cattaruzza F, Hurlbut D, Vanner S, Bunnett N, Vergnolle N. Brain-gut interactions increase peripheral nociceptive signaling in mice with postinfectious irritable bowel syndrome. Gastroenterology. 2011; 141: 2098-108. https://doi.org/10.1053/j.gastro.2011.08.006
26. Ochoa-Cortes F, Guerrero-Alba R, Valdez-Morales EE, Spreadbury I, Barajas-Lopez C, Castro M, Bertrand J, Cenac N, Vergnolle N, Vanner SJ. Chronic stress mediators act synergistically on colonic nociceptive mouse dorsal root ganglia neurons to increase excitability. Neurogastroenterol Motil. 2014; 26: 334-345. https://doi.org/10.1111/nmo.12268
27. Hu S, Xiao Y, Zhu L, Li L, Hu CY, Jiang X, Xu GY. Neonatal maternal deprivation sensitizes voltage-gated sodium channel currents in colon-specific dorsal root ganglion neurons in rats. Am J Physiol Gastrointest Liver Physiol. 2013; 304: G311-21. https://doi.org/10.1152/ajpgi.00338.2012
28. Zemel BM, Ritter DM, Covarrubias M, Muqeem T. A-Type K-V Channels in Dorsal Root Ganglion Neurons: Diversity, Function, and Dysfunction. Front Mol Neurosci. 2018; 11: 253. https://doi.org/10.3389/fnmol.2018.00253
29. Du J, Wang Q, Hu F, Wang J, Ding H, Gao R, Xiao H, Wang L. Effects of estradiol on voltage-gated potassium channels in mouse dorsal root ganglion neurons. J Membr Biol. 2014; 247: 541-8. https://doi.org/10.1007/s00232-014-9670-z
30. Ferrari LF, Khomula EV, Araldi D, Levine JD. Marked Sexual Dimorphism in the Role of the Ryanodine Receptor in a Model of Pain Chronification in the Rat. Sci Rep. 2016; 6: 31221. https://doi.org/10.1038/srep31221
31. Khomula EV, Ferrari LF, Araldi D, Levine JD. 2017. Sexual Dimorphism in a Reciprocal Interaction of Ryanodine and IP_3 Receptors in the Induction of Hyperalgesic Priming. J Neurosci. 37, 2032-2044. https://doi.org/10.1523/JNEUROSCI.2911-16.2017
32. Zhang H, Ding L, Shen T, Peng D. HMGB1 involved in stress-induced depression and its neuroinflammatory priming role: a systematic review. General Psychiatry. 2019; 32: e100084. https://doi.org/10.1136/gpsych-2019-100084.
33. Chen J, Li Q, Saliuk G. Estrogen and serotonin enhance stress-induced visceral hypersensitivity in female rats by up-regulating brain derived neurotrophic factor in spinal cord. 2020. published online ahead of print
34. Ji Y, Tang B, Traub RJ. Spinal estrogen receptor alpha mediates estradiol-induced pronociception in a visceral pain model in the rat. Pain. 2011; 152: 1182-91. https://doi.org/10.1016/j.pain.2011.01.046

Figures

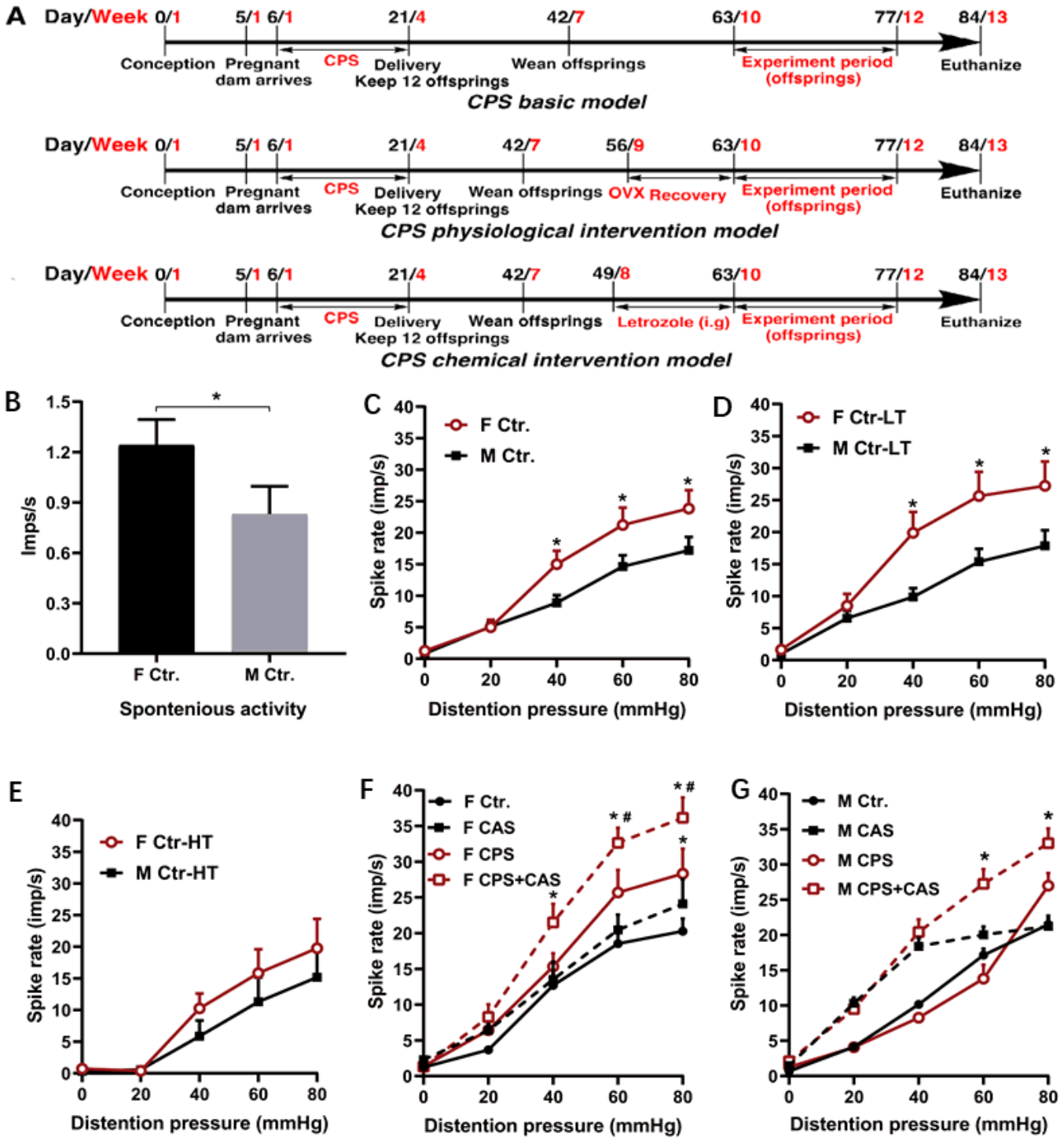

Figure 1

Comparation of primary afferent responses to colorectal distention (CRD). A. Chronic prenatal stress (CPS) plus chronic adult stress (CAS) model. Pregnant dams were subjected to prenatal stress from the 11th day of gestation. Ovariectomy (OVX) or sham surgery was performed on female prenatal stress offspring in the 56th day. Daily Letrozole treatment was initiated on the 49th day, 2 weeks prior to initiation of adult stress. Treatment was continued through the stress protocol. B. Spontaneous activity

(SA) of afferent single units in male and female control rats (n=70 fibers in 6 rats for each group, t-test, *P<0.05). C. Average responses to graded CRD of afferent fibers in male and female control rats (male: n=56 fibers in 6 rats; female: n=70 fibers in 6 rats; two-way ANOVA, *P<0.05 vs. the same pressure male group). D. Responses of low threshold (LT) fibers to CRD in male and female control rats (male: n=42 fibers in 6 rats; female: n=40 fibers in 6 rats; two-way ANOVA, *P<0.05 vs. the same pressure male group). E. Responses of high threshold (HT) afferent fibers to CRD in male and female control rats (male: n=14 fibers in 6 rats; female: n=29 fibers in 6 rats; two-way ANOVA, *P<0.05 vs. the same pressure male group). F. Effects of CAS on afferent fiber responses to CRD from control and CPS female rats (n=6 rats, 59 fibers for control and 99 fibers for CPS female individule group, two-way ANOVA, *P<0.05 vs. the same pressure control group, #P<0.05 vs. the same pressure CPS group). G. Effects of CAS on afferent fiber responses to CRD from control and CPS male rats (n=6 rats, 57 fibers for control and 95 fibers for CPS femalegroup, two-way ANOVA, *P<0.05 vs. the same pressure control group).

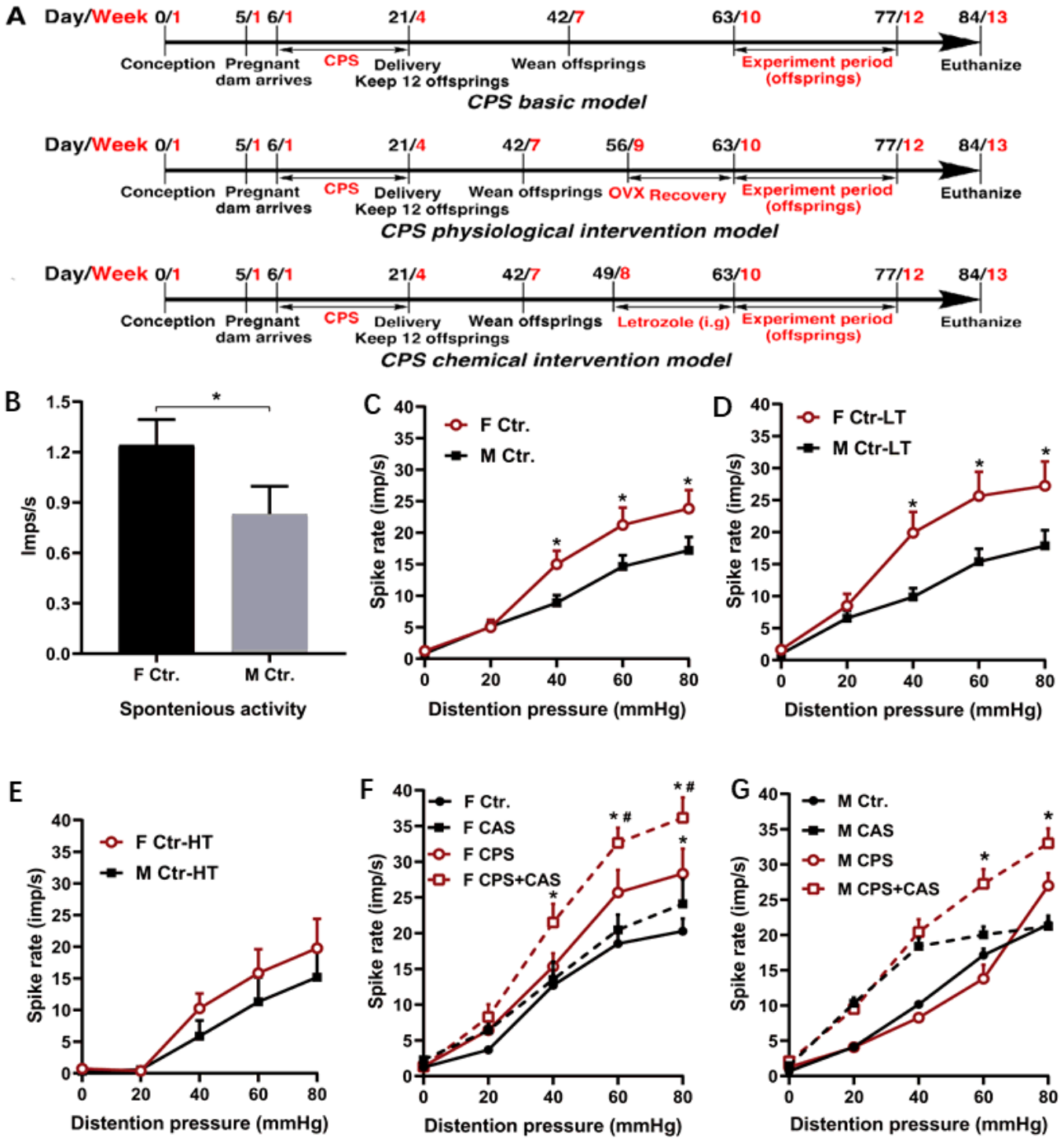

Figure 1

Comparation of primary afferent responses to colorectal distention (CRD). A. Chronic prenatal stress (CPS) plus chronic adult stress (CAS) model. Pregnant dams were subjected to prenatal stress from the 11th day of gestation. Ovariectomy (OVX) or sham surgery was performed on female prenatal stress offspring in the 56th day. Daily Letrozole treatment was initiated on the 49th day, 2 weeks prior to initiation of adult stress. Treatment was continued through the stress protocol. B. Spontaneous activity

(SA) of afferent single units in male and female control rats (n=70 fibers in 6 rats for each group, t-test, *P<0.05). C. Average responses to graded CRD of afferent fibers in male and female control rats (male: n=56 fibers in 6 rats; female: n=70 fibers in 6 rats; two-way ANOVA, *P<0.05 vs. the same pressure male group). D. Responses of low threshold (LT) fibers to CRD in male and female control rats (male: n=42 fibers in 6 rats; female: n=40 fibers in 6 rats; two-way ANOVA, *P<0.05 vs. the same pressure male group). E. Responses of high threshold (HT) afferent fibers to CRD in male and female control rats (male: n=14 fibers in 6 rats; female: n=29 fibers in 6 rats; two-way ANOVA, *P<0.05 vs. the same pressure male group). F. Effects of CAS on afferent fiber responses to CRD from control and CPS female rats (n=6 rats, 59 fibers for control and 99 fibers for CPS female individule group, two-way ANOVA, *P<0.05 vs. the same pressure control group, #P<0.05 vs. the same pressure CPS group). G. Effects of CAS on afferent fiber responses to CRD from control and CPS male rats (n=6 rats, 57 fibers for control and 95 fibers for CPS femalegroup, two-way ANOVA, *P<0.05 vs. the same pressure control group).

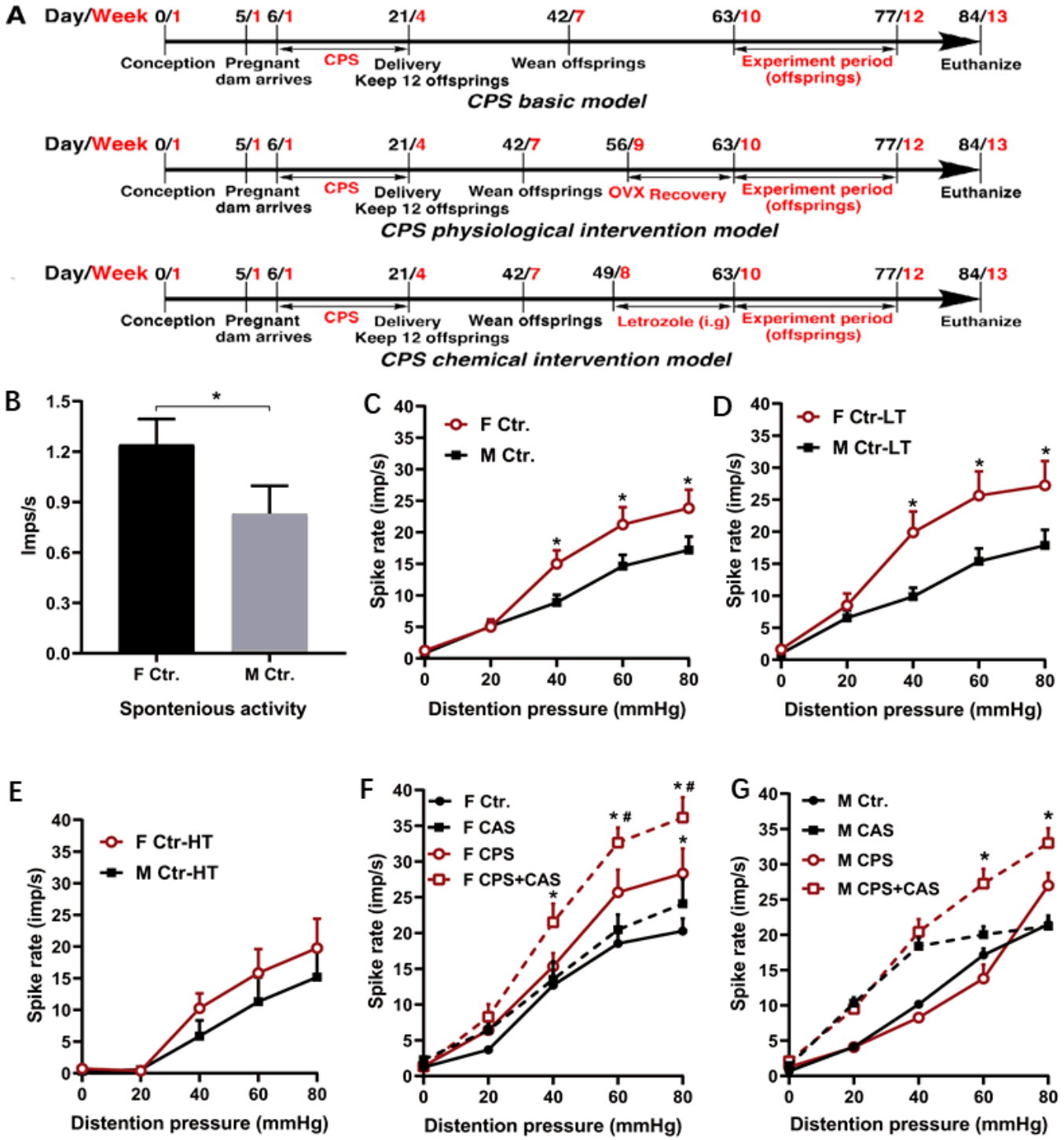

Figure 1

Comparation of primary afferent responses to colorectal distention (CRD). A. Chronic prenatal stress (CPS) plus chronic adult stress (CAS) model. Pregnant dams were subjected to prenatal stress from the 11th day of gestation. Ovariectomy (OVX) or sham surgery was performed on female prenatal stress offspring in the 56th day. Daily Letrozole treatment was initiated on the 49th day, 2 weeks prior to initiation of adult stress. Treatment was continued through the stress protocol. B. Spontaneous activity

(SA) of afferent single units in male and female control rats (n=70 fibers in 6 rats for each group, t-test, *P<0.05). C. Average responses to graded CRD of afferent fibers in male and female control rats (male: n=56 fibers in 6 rats; female: n=70 fibers in 6 rats; two-way ANOVA, *P<0.05 vs. the same pressure male group). D. Responses of low threshold (LT) fibers to CRD in male and female control rats (male: n=42 fibers in 6 rats; female: n=40 fibers in 6 rats; two-way ANOVA, *P<0.05 vs. the same pressure male group). E. Responses of high threshold (HT) afferent fibers to CRD in male and female control rats (male: n=14 fibers in 6 rats; female: n=29 fibers in 6 rats; two-way ANOVA, *P<0.05 vs. the same pressure male group). F. Effects of CAS on afferent fiber responses to CRD from control and CPS female rats (n=6 rats, 59 fibers for control and 99 fibers for CPS female individule group, two-way ANOVA, *P<0.05 vs. the same pressure control group, #P<0.05 vs. the same pressure CPS group). G. Effects of CAS on afferent fiber responses to CRD from control and CPS male rats (n=6 rats, 57 fibers for control and 95 fibers for CPS femalegroup, two-way ANOVA, *P<0.05 vs. the same pressure control group).

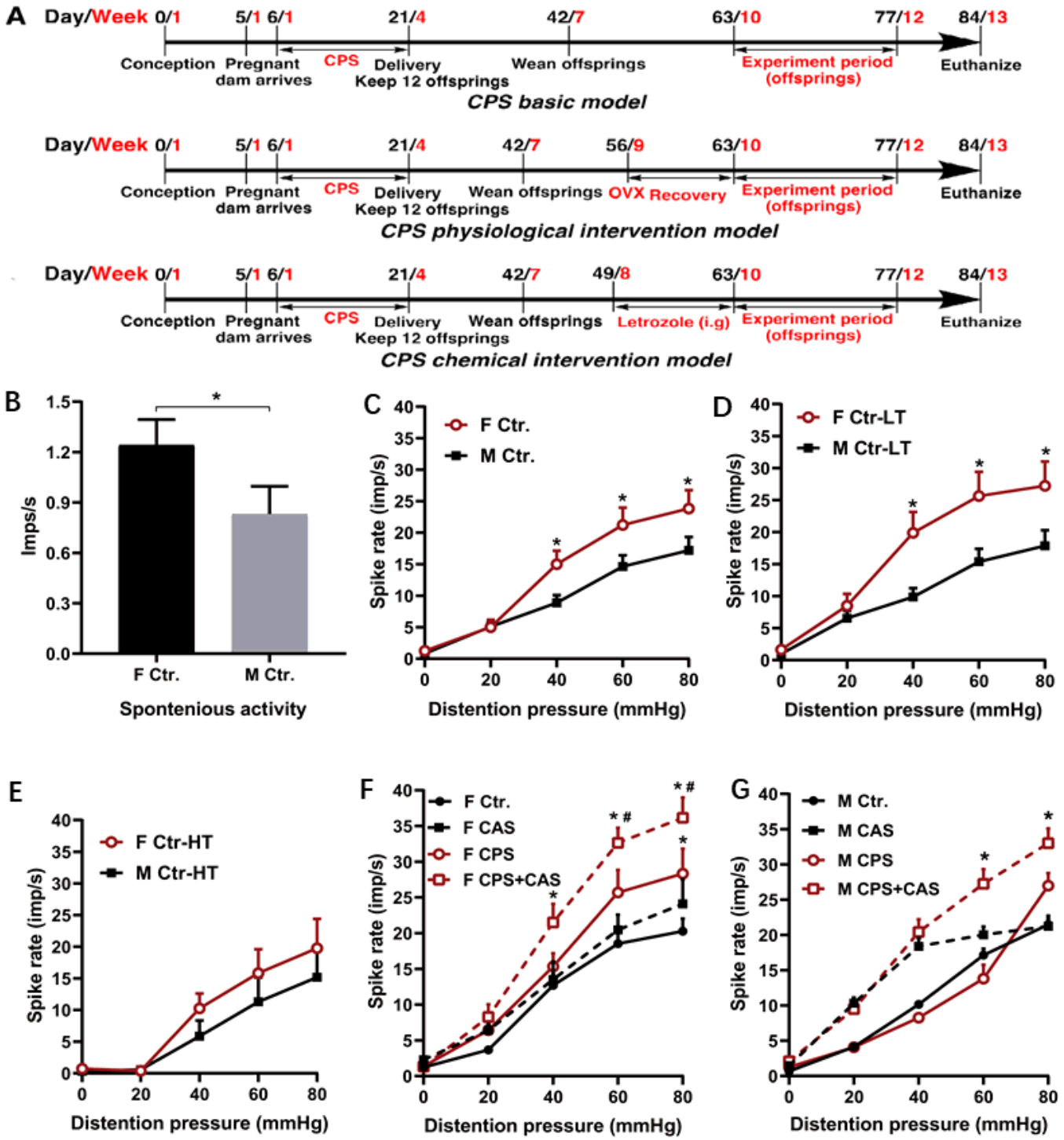

Figure 1

Comparation of primary afferent responses to colorectal distention (CRD). A. Chronic prenatal stress (CPS) plus chronic adult stress (CAS) model. Pregnant dams were subjected to prenatal stress from the 11th day of gestation. Ovariectomy (OVX) or sham surgery was performed on female prenatal stress offspring in the 56th day. Daily Letrozole treatment was initiated on the 49th day, 2 weeks prior to initiation of adult stress. Treatment was continued through the stress protocol. B. Spontaneous activity

(SA) of afferent single units in male and female control rats (n=70 fibers in 6 rats for each group, t-test, *P<0.05). C. Average responses to graded CRD of afferent fibers in male and female control rats (male: n=56 fibers in 6 rats; female: n=70 fibers in 6 rats; two-way ANOVA, *P<0.05 vs. the same pressure male group). D. Responses of low threshold (LT) fibers to CRD in male and female control rats (male: n=42 fibers in 6 rats; female: n=40 fibers in 6 rats; two-way ANOVA, *P<0.05 vs. the same pressure male group). E. Responses of high threshold (HT) afferent fibers to CRD in male and female control rats (male: n=14 fibers in 6 rats; female: n=29 fibers in 6 rats; two-way ANOVA, *P<0.05 vs. the same pressure male group). F. Effects of CAS on afferent fiber responses to CRD from control and CPS female rats (n=6 rats, 59 fibers for control and 99 fibers for CPS female individule group, two-way ANOVA, *P<0.05 vs. the same pressure control group, #P<0.05 vs. the same pressure CPS group). G. Effects of CAS on afferent fiber responses to CRD from control and CPS male rats (n=6 rats, 57 fibers for control and 95 fibers for CPS femalegroup, two-way ANOVA, *P<0.05 vs. the same pressure control group).

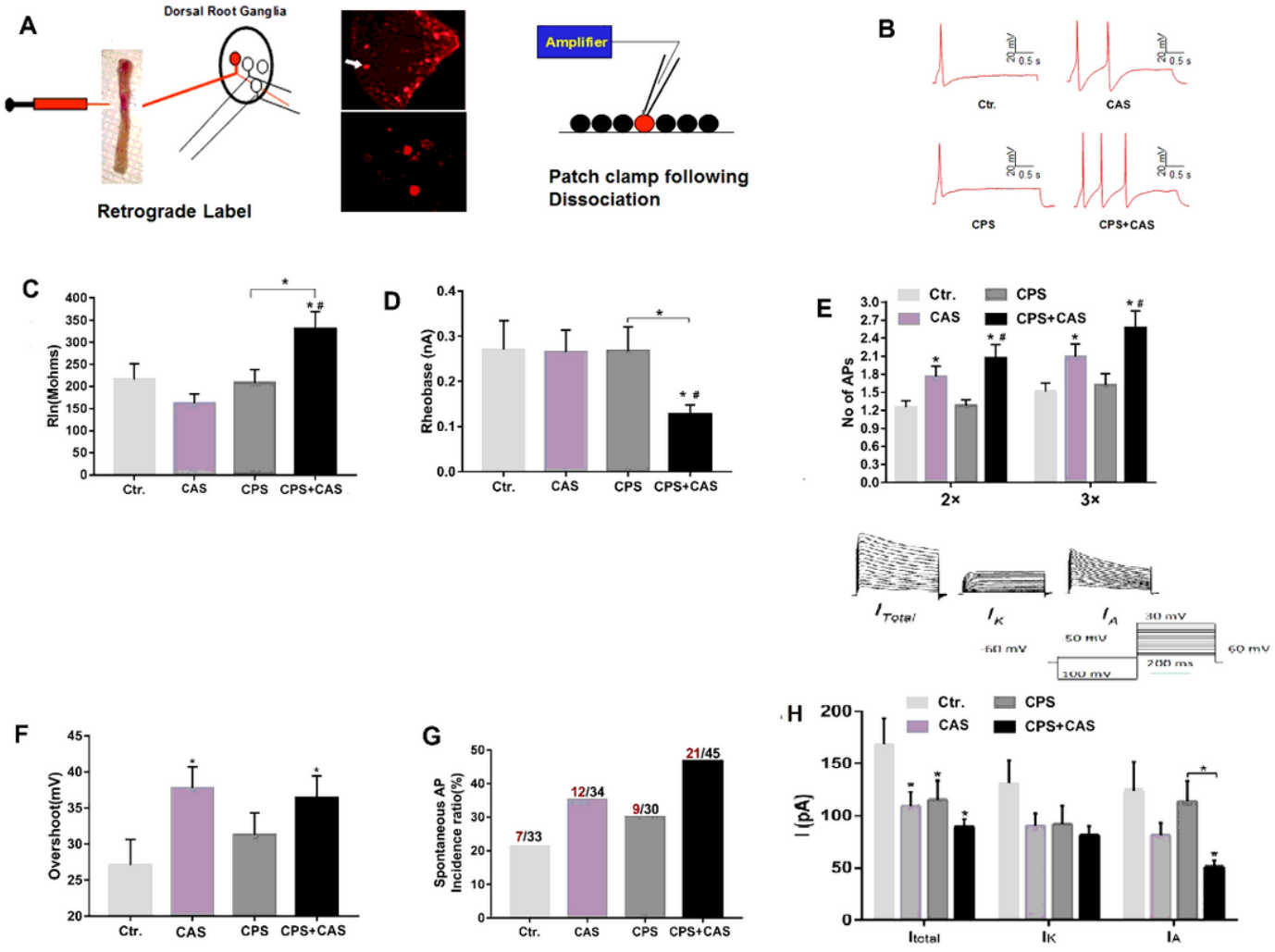

Figure 2

Patch clamp recording in colonic DRG neurons from female rats. A. Patch clamp process of cell labeling. Under isoflurane anesthesia, the lipid soluble fluorescent 9-DiI was injected into muscularis externae on

the exposed distal colon. Lumbosacral (L6–S2) DRGs (A. middle up picture) were isolated and DiI labeled neurons were identified under fluorescent microscope (A. middle down picture). Electrophysiological properties of each neuron were measured using whole-cell current and voltage clamp protocols (A. right figure). B. Representative action potentials elicited by current injection at 2X the rheobase in neurons from control, chronic adult stress (CAS), chronic prenatal stress (CPS) and CPS+ CAS female rats. C. Membrane input resistance from all four groups (n=5 rats, 45 cells in each group, one-way ANOVA, *P<0.05 vs. control, #P<0.05 vs. CPS). D. Rheobase from all four experimental groups (n=5 rats, 45 cells in each group, one-way ANOVA, *P<0.05 vs. control or as the graph shown, #P<0.05 vs. CAS). E. Number of action potentials elicited by current injection at either 2x and 3x the rheobase in all four experimental groups (two-way ANOVA, *P<0.05 vs. control, #P<0.05 vs. CPS). F. Action potential overshoot recorded from all four experimental groups (*P<0.05 vs. control). G. The proportion of neurons from each experimental group exhibiting spontaneous action potentials. Red numbers represent spontaneous AP firing cells, as well as black numbers represent total cells. H. Representative total, IK and IA current tracings and average values of potassium currents: Itotal, IK and IA were shown (female CPS + CAS, CAS, CPS (n=15 neurons, from 5 rats in each group), and control groups (n=12 neurons from 5 rats) two-way ANOVA, *P<0.05 vs. each control group or as the right graph shown).

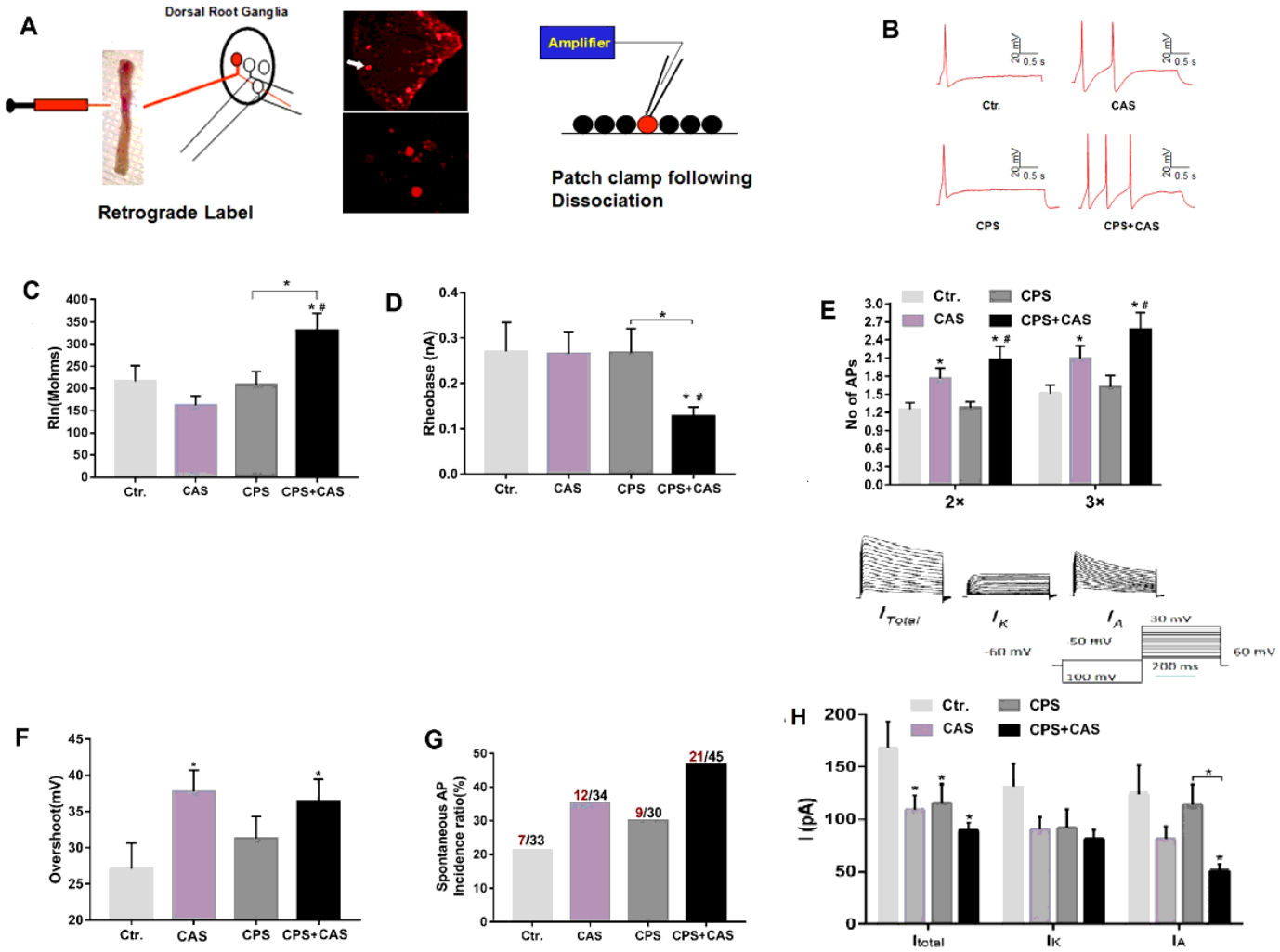

Figure 2

Patch clamp recording in colonic DRG neurons from female rats. A. Patch clamp process of cell labeling. Under isoflurane anesthesia, the lipid soluble fluorescent 9-DiI was injected into muscularis externae on the exposed distal colon. Lumbosacral (L6–S2) DRGs (A. middle up picture) were isolated and DiI labeled neurons were identified under fluorescent microscope (A. middle down picture). Electrophysiological properties of each neuron were measured using whole-cell current and voltage clamp protocols (A. right figure). B. Representative action potentials elicited by current injection at 2X the rheobase in neurons from control, chronic adult stress (CAS), chronic prenatal stress (CPS) and CPS+ CAS female rats. C. Membrane input resistance from all four groups (n=5 rats, 45 cells in each group, one-way ANOVA, *P<0.05 vs. control, #P<0.05 vs. CPS). D. Rheobase from all four experimental groups (n=5 rats, 45 cells in each group, one-way ANOVA, *P<0.05 vs. control or as the graph shown, #P<0.05 vs. CAS). E. Number of action potentials elicited by current injection at either 2x and 3x the rheobase in all four experimental groups (two-way ANOVA, *P<0.05 vs. control, #P<0.05 vs. CPS). F. Action potential overshoot recorded from all four experimental groups (*P<0.05 vs. control). G. The proportion of neurons from each experimental group exhibiting spontaneous action potentials. Red numbers represent spontaneous AP firing cells, as well as black numbers represent total cells. H. Representative total, IK and IA current tracings and average values of potassium currents: Itotal, IK and IA were shown (female CPS + CAS, CAS, CPS (n=15 neurons, from 5 rats in each group), and control groups (n=12 neurons from 5 rats) two-way ANOVA, *P<0.05 vs. each control group or as the right graph shown).

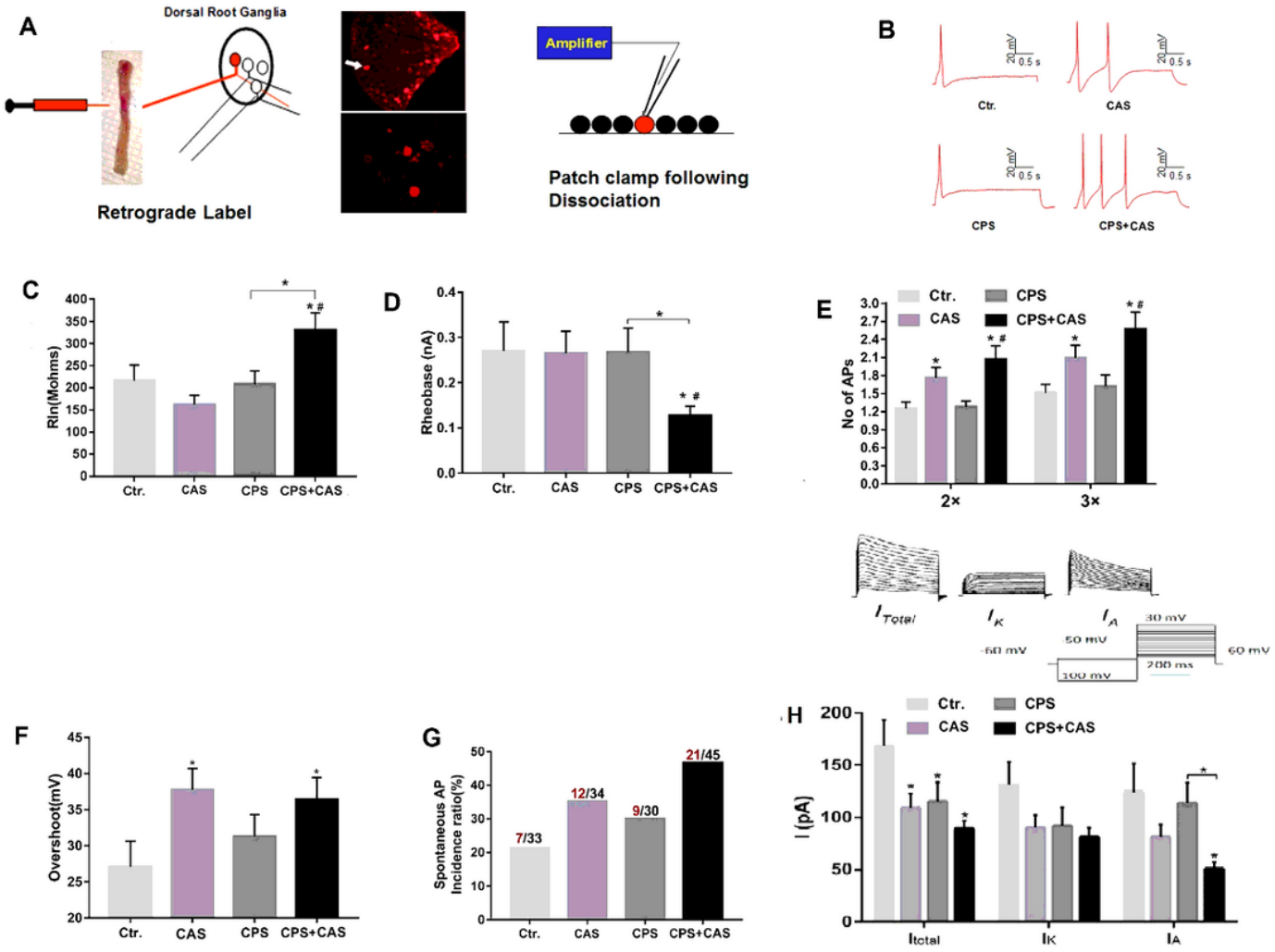

Figure 2

Patch clamp recording in colonic DRG neurons from female rats. A. Patch clamp process of cell labeling. Under isoflurane anesthesia, the lipid soluble fluorescent 9-DiI was injected into muscularis externae on the exposed distal colon. Lumbosacral (L6–S2) DRGs (A. middle up picture) were isolated and DiI labeled neurons were identified under fluorescent microscope (A. middle down picture). Electrophysiological properties of each neuron were measured using whole-cell current and voltage clamp protocols (A. right figure). B. Representative action potentials elicited by current injection at 2X the rheobase in neurons from control, chronic adult stress (CAS), chronic prenatal stress (CPS) and CPS+ CAS female rats. C. Membrane input resistance from all four groups (n=5 rats, 45 cells in each group, one-way ANOVA, *P<0.05 vs. control, #P<0.05 vs. CPS). D. Rheobase from all four experimental groups (n=5 rats, 45 cells in each group, one-way ANOVA, *P<0.05 vs. control or as the graph shown, #P<0.05 vs. CAS). E. Number of action potentials elicited by current injection at either 2x and 3x the rheobase in all four experimental groups (two-way ANOVA, *P<0.05 vs. control, #P<0.05 vs. CPS). F. Action potential overshoot recorded from all four experimental groups (*P<0.05 vs. control). G. The proportion of neurons from each experimental group exhibiting spontaneous action potentials. Red numbers represent spontaneous AP

firing cells, as well as black numbers represent total cells. H. Representative total, IK and IA current tracings and average values of potassium currents: Itotal, IK and IA were shown (female CPS + CAS, CAS, CPS (n=15 neurons, from 5 rats in each group), and control groups (n=12 neurons from 5 rats) two-way ANOVA, *P<0.05 vs. each control group or as the right graph shown).

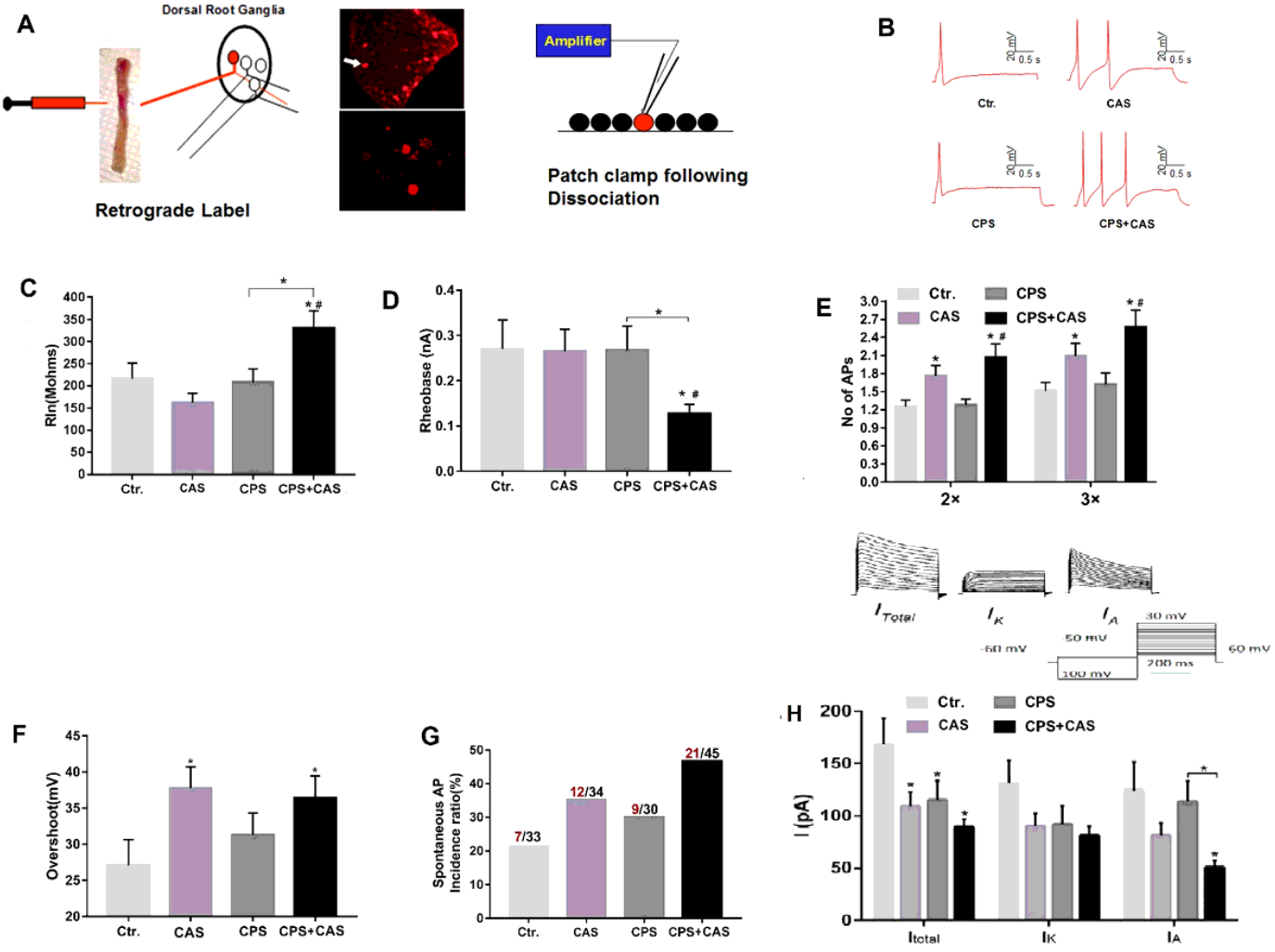

Figure 2

Patch clamp recording in colonic DRG neurons from female rats. A. Patch clamp process of cell labeling. Under isoflurane anesthesia, the lipid soluble fluorescent 9-DiI was injected into muscularis externae on the exposed distal colon. Lumbosacral (L6–S2) DRGs (A. middle up picture) were isolated and DiI labeled neurons were identified under fluorescent microscope (A. middle down picture). Electrophysiological properties of each neuron were measured using whole-cell current and voltage clamp protocols (A. right figure). B. Representative action potentials elicited by current injection at 2X the rheobase in neurons from control, chronic adult stress (CAS), chronic prenatal stress (CPS) and CPS+ CAS female rats. C. Membrane input resistance from all four groups (n=5 rats, 45 cells in each group, one-way ANOVA, *P<0.05 vs. control, #P<0.05 vs. CPS). D. Rheobase from all four experimental groups (n=5 rats, 45 cells in each group, one-way ANOVA, *P<0.05 vs. control or as the graph shown, #P<0.05 vs. CAS). E. Number

of action potentials elicited by current injection at either 2x and 3x the rheobase in all four experimental groups (two-way ANOVA, *P<0.05 vs. control, #P<0.05 vs. CPS). F. Action potential overshoot recorded from all four experimental groups (*P<0.05 vs. control). G. The proportion of neurons from each experimental group exhibiting spontaneous action potentials. Red numbers represent spontaneous AP firing cells, as well as black numbers represent total cells. H. Representative total, IK and IA current tracings and average values of potassium currents: Itotal, IK and IA were shown (female CPS + CAS, CAS, CPS (n=15 neurons, from 5 rats in each group), and control groups (n=12 neurons from 5 rats) two-way ANOVA, *P<0.05 vs. each control group or as the right graph shown).

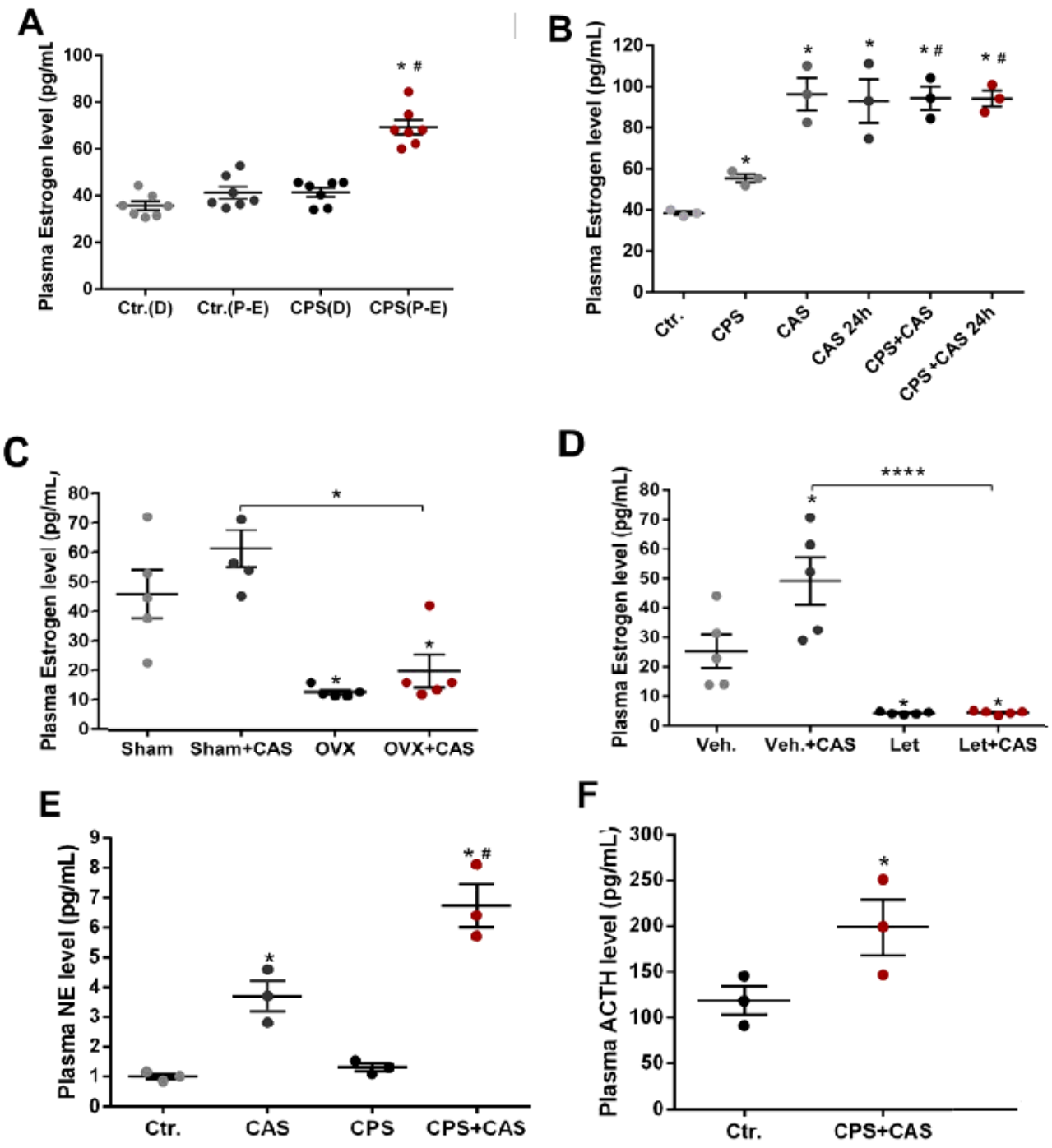

Figure 3

Effects of chronic prenatal stress (CPS), chronic adult stress (CAS), ovariectomy (OVX) and letrozole treatment on plasma estrogen levels in female rats. A. Plasma estrogen level changes in control and CPS rats by estrus cycle phases (n=8 rats, one-way ANOVA, *P<0.05 vs. control proestrus/estrus (P-E) phase, #P<0.05 vs. CPS diestrus (D) phase).B. Plasma estrogen levels increase in CPS rats and following CAS 24 hours after last adult stressor (n=8 rats, one-way ANOVA, *P<0.05 vs. control, #P<0.05 vs. CPS). C.

OVX significantly reduced CPS female rat plasma estrogen levels before and after CAS (n=5 rats, one-way ANOVA, *P<0.05 vs. sham group or as the graph shown). D. Letrozole treatment significantly reduced CPS female rat plasma estrogen levels before or after CAS (n=5 rats, one-way ANOVA,*P<0.05 vs. vehicle group or as the graph shown). E. Plasma norepinephrine (NE) levels from control, CAS, CPS and CPS+CAS group female rats (n=5 rats, one-way ANOVA, *P<0.05 vs. control, #P<0.05 vs. CPS). F. Plasma adrenocorticotropic hormone (ACTH) levels from control and CPS+CAS group female rats (n=5 rats, t-test, *P<0.05 vs. control).

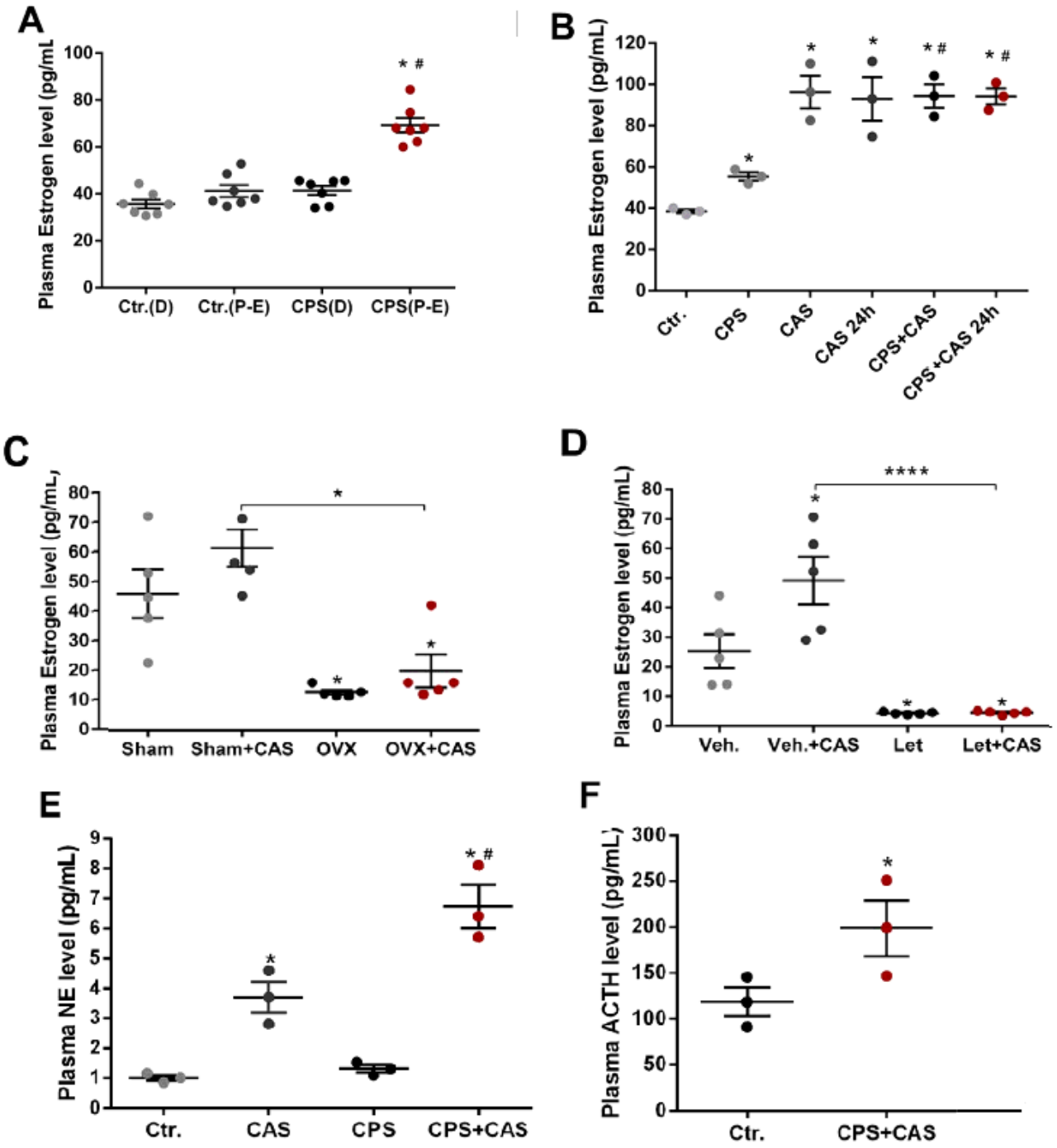

Figure 3

Effects of chronic prenatal stress (CPS), chronic adult stress (CAS), ovariectomy (OVX) and letrozole treatment on plasma estrogen levels in female rats. A. Plasma estrogen level changes in control and CPS rats by estrus cycle phases (n=8 rats, one-way ANOVA, *P<0.05 vs. control proestrus/estrus (P-E) phase, #P<0.05 vs. CPS diestrus (D) phase).B. Plasma estrogen levels increase in CPS rats and following CAS 24 hours after last adult stressor (n=8 rats, one-way ANOVA, *P<0.05 vs. control, #P<0.05 vs. CPS). C. OVX significantly reduced CPS female rat plasma estrogen levels before and after CAS (n=5 rats, one-way ANOVA, *P<0.05 vs. sham group or as the graph shown). D. Letrozole treatment significantly reduced CPS female rat plasma estrogen levels before or after CAS (n=5 rats, one-way ANOVA,*P<0.05 vs. vehicle group or as the graph shown). E. Plasma norepinephrine (NE) levels from control, CAS, CPS and CPS+CAS group female rats (n=5 rats, one-way ANOVA, *P<0.05 vs. control, #P<0.05 vs. CPS). F. Plasma adrenocorticotropic hormone (ACTH) levels from control and CPS+CAS group female rats (n=5 rats, t-test, *P<0.05 vs. control).

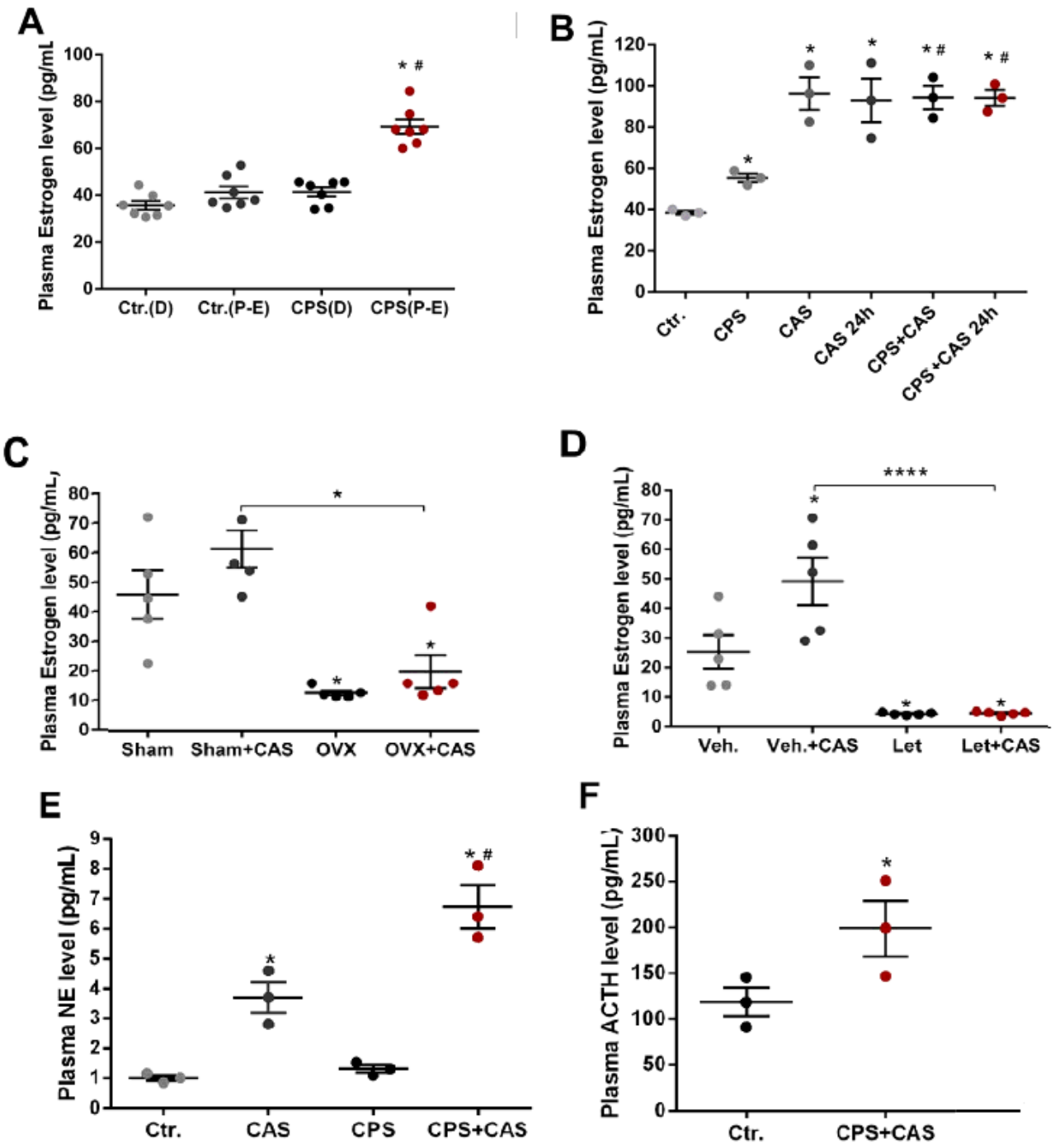

Figure 3

Effects of chronic prenatal stress (CPS), chronic adult stress (CAS), ovariectomy (OVX) and letrozole treatment on plasma estrogen levels in female rats. A. Plasma estrogen level changes in control and CPS rats by estrus cycle phases (n=8 rats, one-way ANOVA, *P<0.05 vs. control proestrus/estrus (P-E) phase, #P<0.05 vs. CPS diestrus (D) phase).B. Plasma estrogen levels increase in CPS rats and following CAS 24 hours after last adult stressor (n=8 rats, one-way ANOVA, *P<0.05 vs. control, #P<0.05 vs. CPS). C.

OVX significantly reduced CPS female rat plasma estrogen levels before and after CAS (n=5 rats, one-way ANOVA, *P<0.05 vs. sham group or as the graph shown). D. Letrozole treatment significantly reduced CPS female rat plasma estrogen levels before or after CAS (n=5 rats, one-way ANOVA,*P<0.05 vs. vehicle group or as the graph shown). E. Plasma norepinephrine (NE) levels from control, CAS, CPS and CPS+CAS group female rats (n=5 rats, one-way ANOVA, *P<0.05 vs. control, #P<0.05 vs. CPS). F. Plasma adrenocorticotropic hormone (ACTH) levels from control and CPS+CAS group female rats (n=5 rats, t-test, *P<0.05 vs. control).

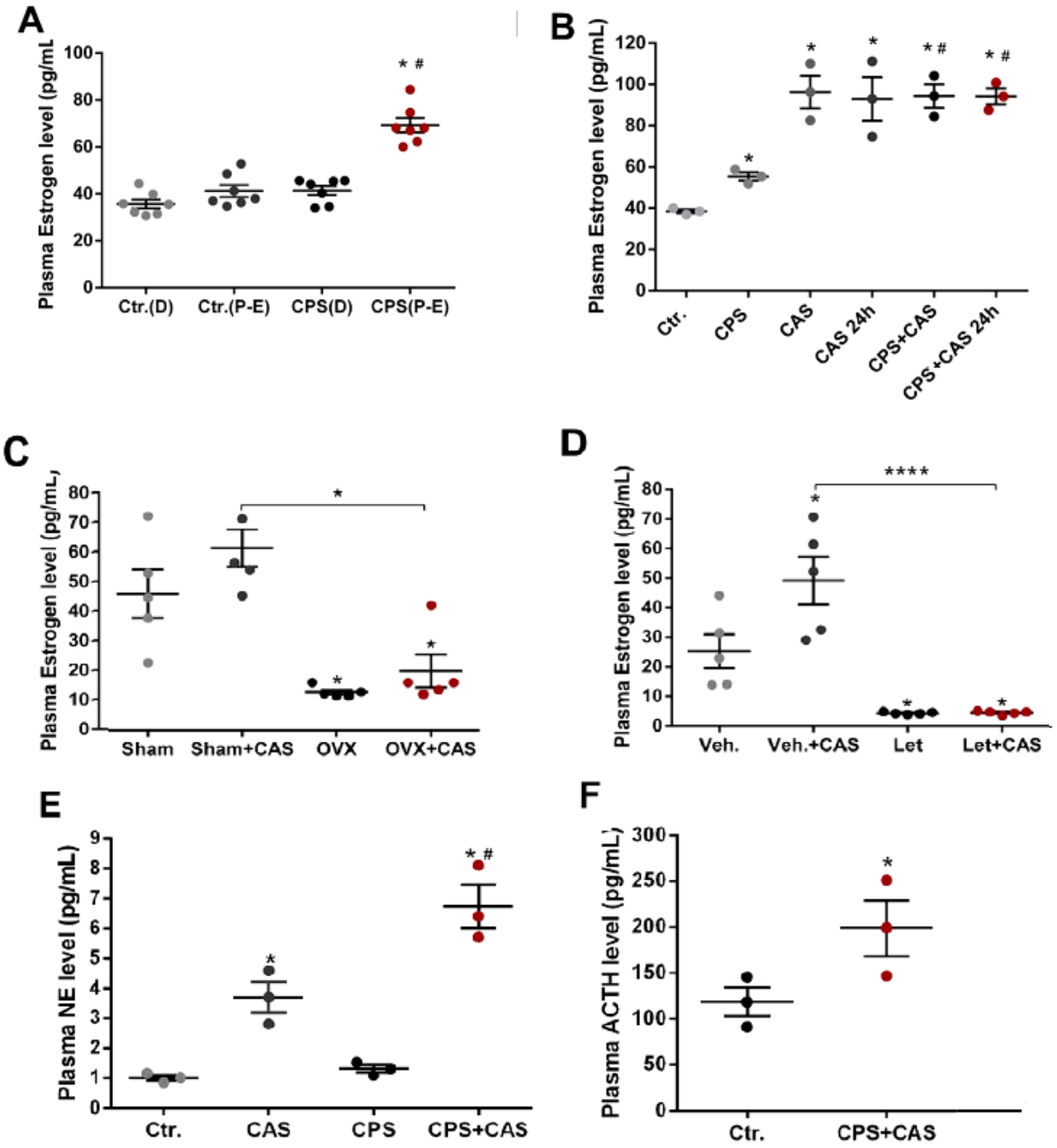

Figure 3

Effects of chronic prenatal stress (CPS), chronic adult stress (CAS), ovariectomy (OVX) and letrozole treatment on plasma estrogen levels in female rats. A. Plasma estrogen level changes in control and CPS rats by estrus cycle phases (n=8 rats, one-way ANOVA, *P<0.05 vs. control proestrus/estrus (P-E) phase, #P<0.05 vs. CPS diestrus (D) phase).B. Plasma estrogen levels increase in CPS rats and following CAS 24 hours after last adult stressor (n=8 rats, one-way ANOVA, *P<0.05 vs. control, #P<0.05 vs. CPS). C. OVX significantly reduced CPS female rat plasma estrogen levels before and after CAS (n=5 rats, one-way ANOVA, *P<0.05 vs. sham group or as the graph shown). D. Letrozole treatment significantly reduced CPS female rat plasma estrogen levels before or after CAS (n=5 rats, one-way ANOVA,*P<0.05 vs. vehicle group or as the graph shown). E. Plasma norepinephrine (NE) levels from control, CAS, CPS and CPS+CAS group female rats (n=5 rats, one-way ANOVA, *P<0.05 vs. control, #P<0.05 vs. CPS). F. Plasma adrenocorticotropic hormone (ACTH) levels from control and CPS+CAS group female rats (n=5 rats, t-test, *P<0.05 vs. control).

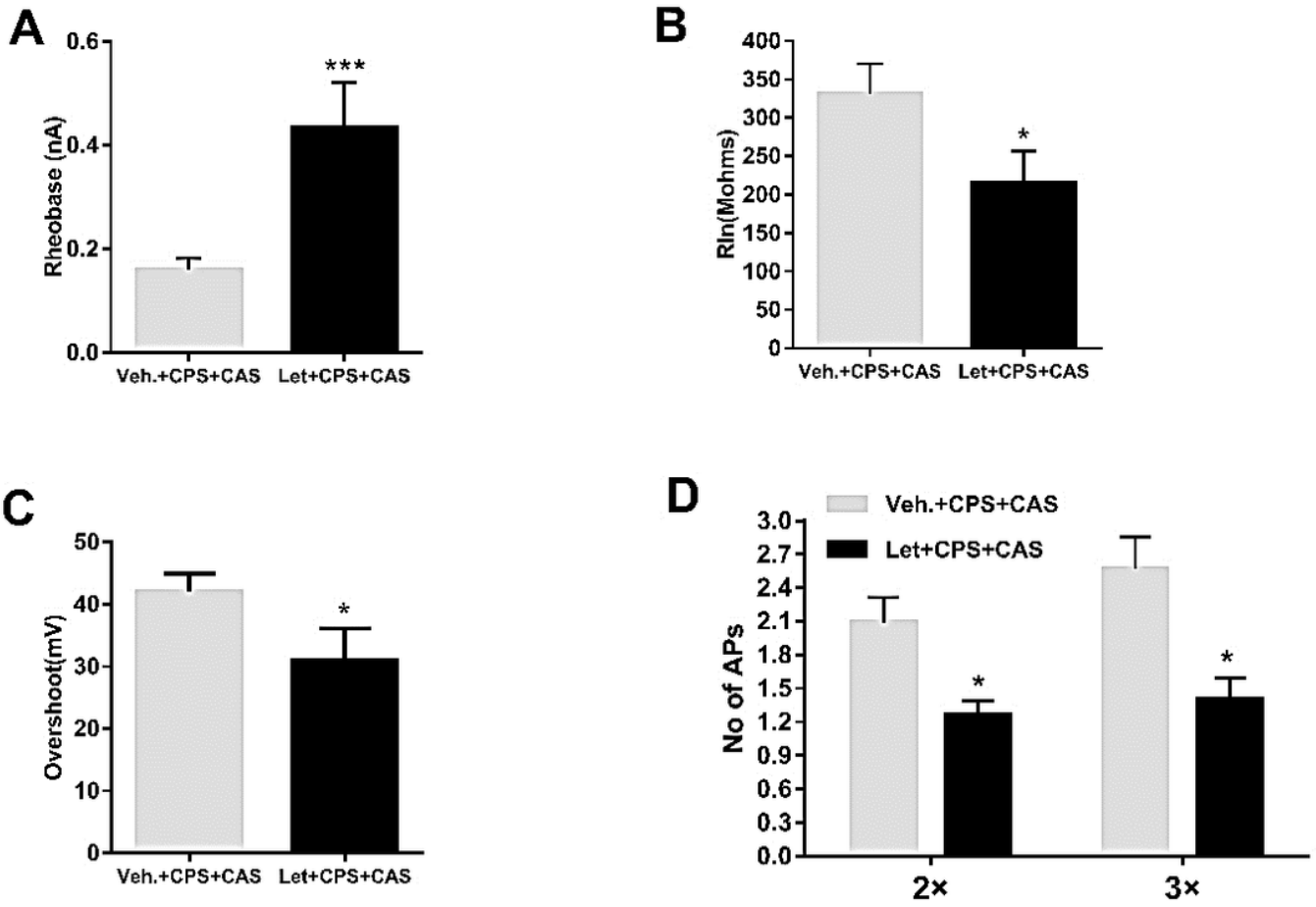

Figure 4

Effects of Letrozole treatment on colon DRG neuron excitability. A. Rheobase (n=45 cells in 6 rats in each group, t-test, ***P<0.0001 vs. Veh.+CAS+CPS). B. Membrane input resistance (RIn) (t-test, *P<0.05). C.

Action potential overshoot (t-test, *P<0.05). D. Number of action potentials (APs) elicited by current injection at 2x and 3x rheobase (two-way ANOVA, *P<0.05).

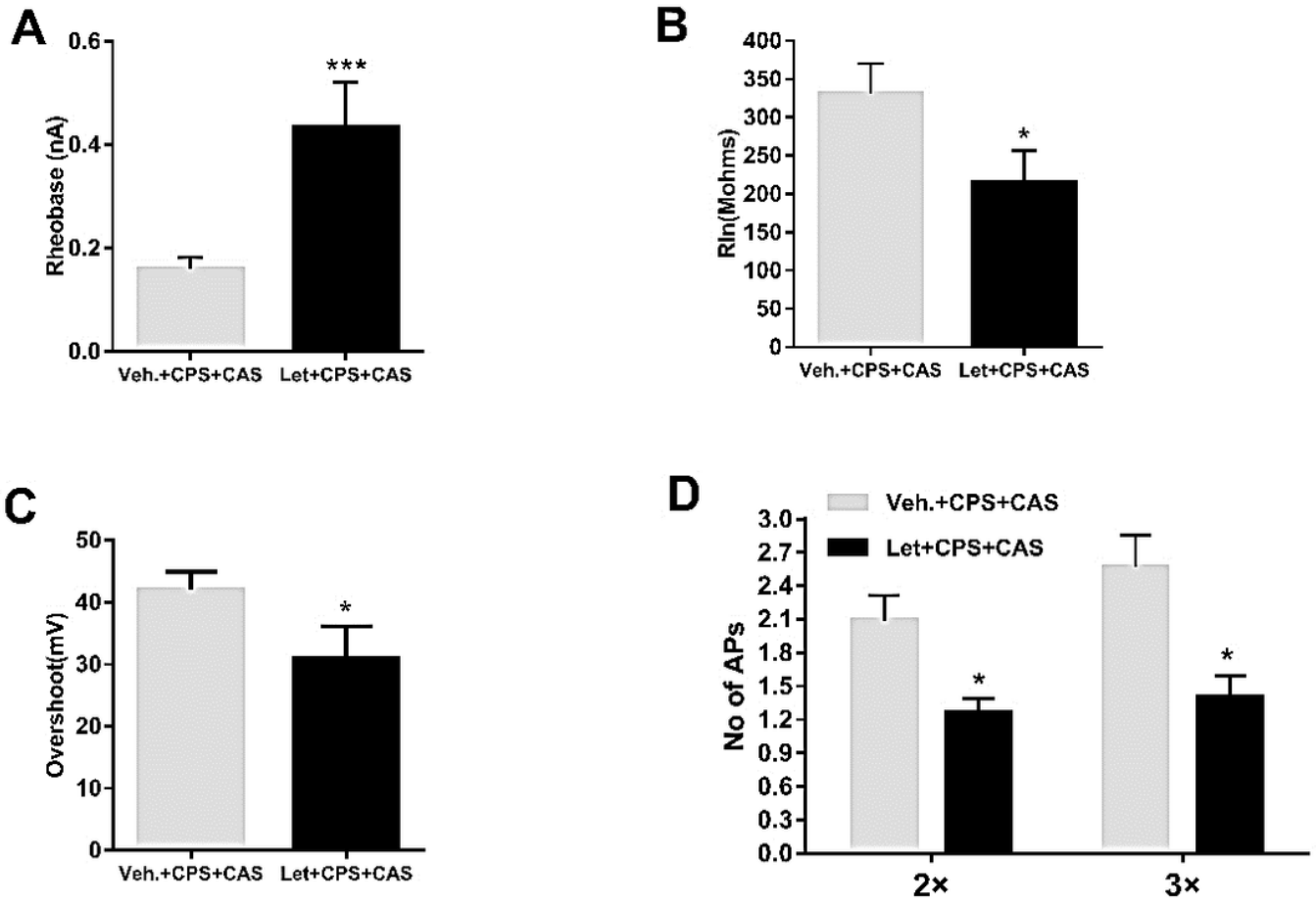

Figure 4

Effects of Letrozole treatment on colon DRG neuron excitability. A. Rheobase (n=45 cells in 6 rats in each group, t-test, ***P<0.0001 vs. Veh.+CAS+CPS). B. Membrane input resistance (Rin) (t-test, *P<0.05). C. Action potential overshoot (t-test, *P<0.05). D. Number of action potentials (APs) elicited by current injection at 2x and 3x rheobase (two-way ANOVA, *P<0.05).

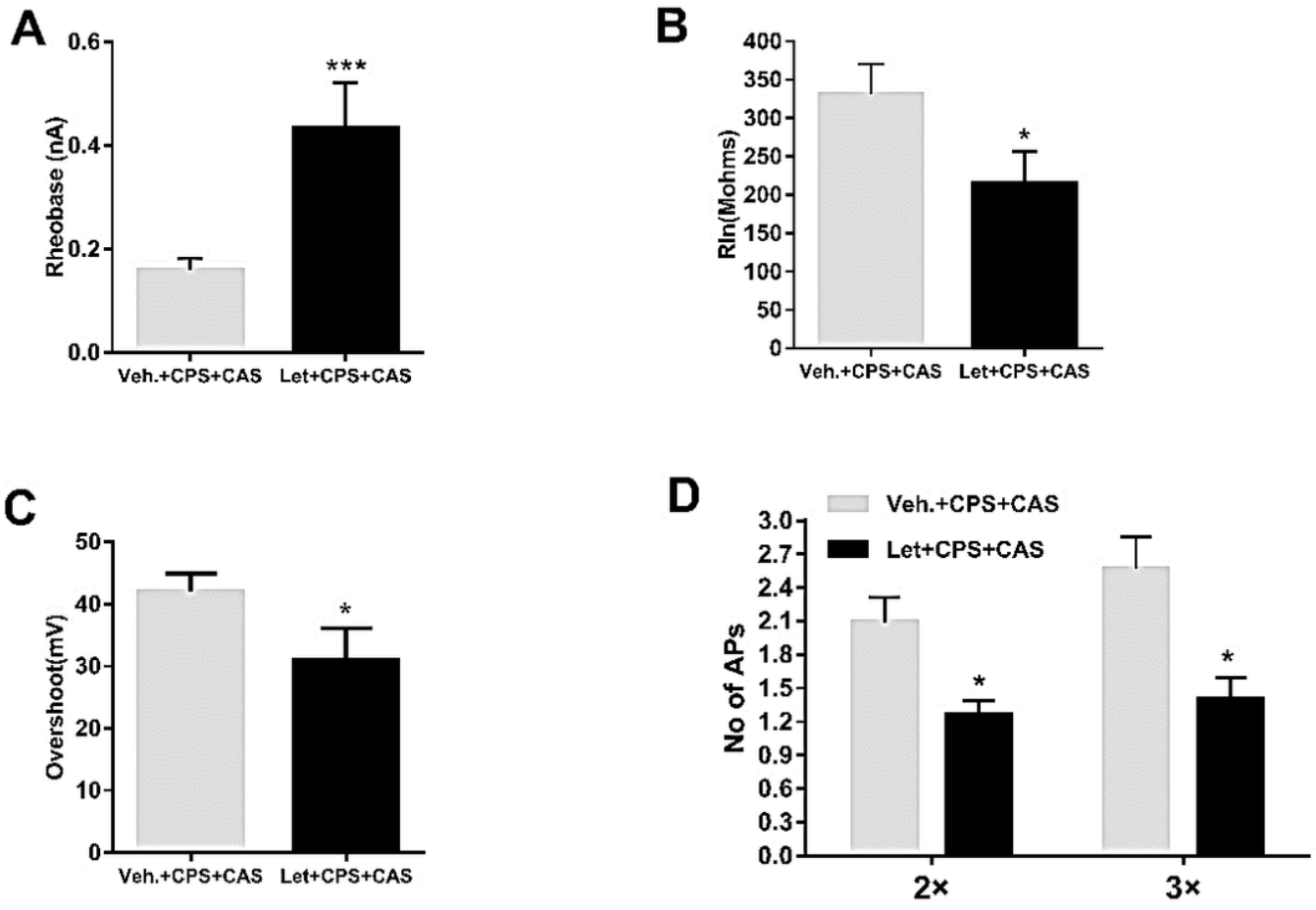

Figure 4

Effects of Letrozole treatment on colon DRG neuron excitability. A. Rheobase (n=45 cells in 6 rats in each group, t-test, ***P<0.0001 vs. Veh.+CAS+CPS). B. Membrane input resistance (Rin) (t-test, *P<0.05). C. Action potential overshoot (t-test, *P<0.05). D. Number of action potentials (APs) elicited by current injection at 2x and 3x rheobase (two-way ANOVA, *P<0.05).

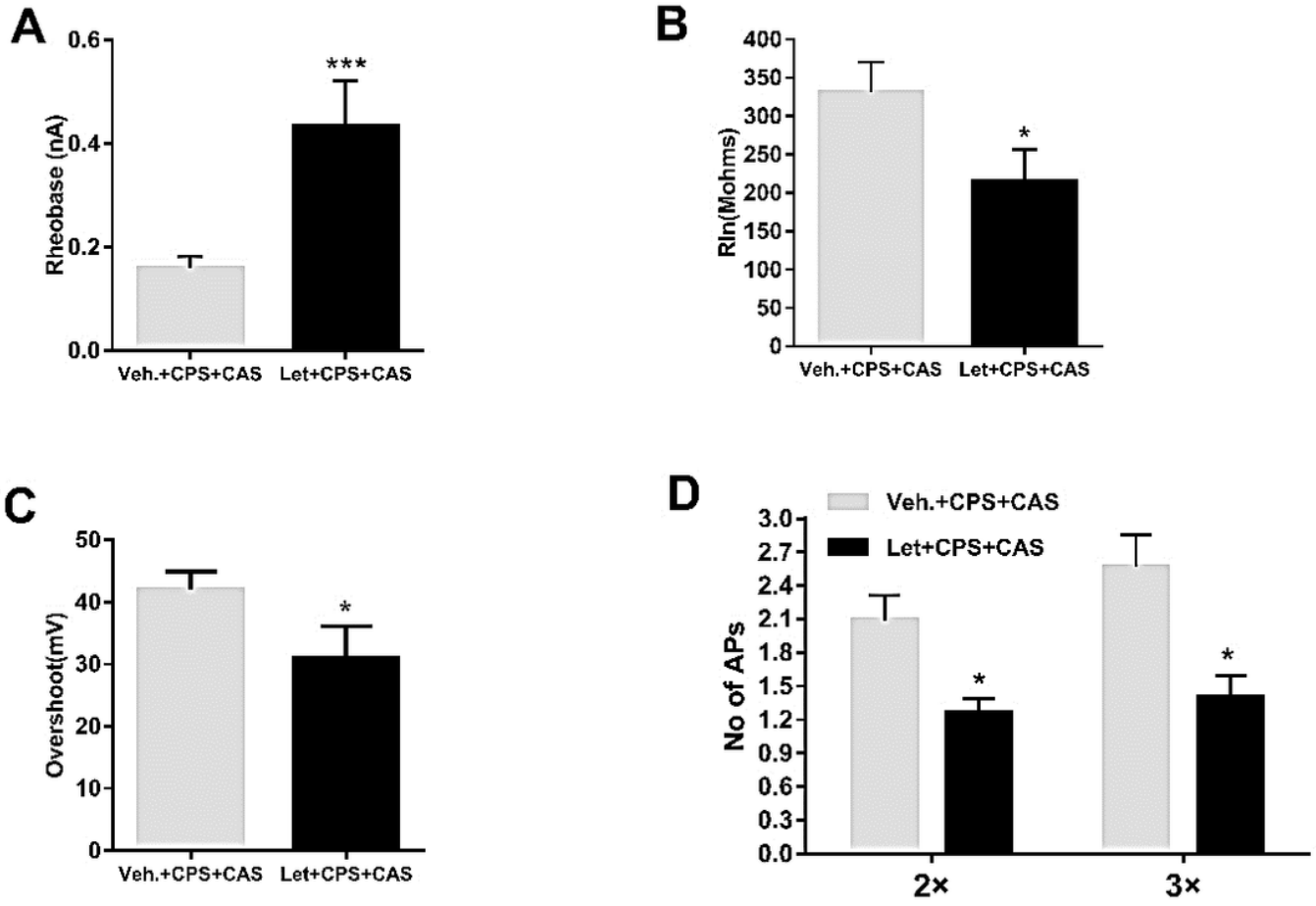

Figure 4

Effects of Letrozole treatment on colon DRG neuron excitability. A. Rheobase (n=45 cells in 6 rats in each group, t-test, ***P<0.0001 vs. Veh.+CAS+CPS). B. Membrane input resistance (Rin) (t-test, *P<0.05). C. Action potential overshoot (t-test, *P<0.05). D. Number of action potentials (APs) elicited by current injection at 2x and 3x rheobase (two-way ANOVA, *P<0.05).

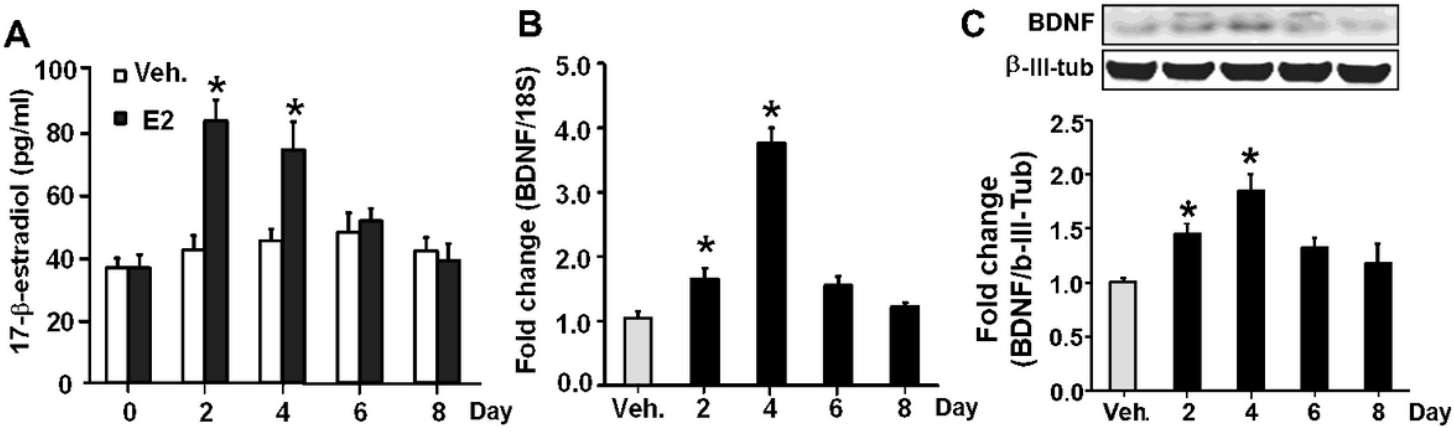

Figure 5

BDNF expression in lumbar-sacral spinal cord is regulated by estrogen. A. Plasma estrogen levels in cycling females that received a bolus estradiol (E2) infusion on day 1 (n= 8 rats in each group, two-way ANOVA, *P<0.05 vs. vehicle group). B. Lumbar sacral spinal cord BDNF mRNA following bolus estrogen infusion. C. Lumbar sacral spinal cord BDNF protein following bolus estrogen infusion.

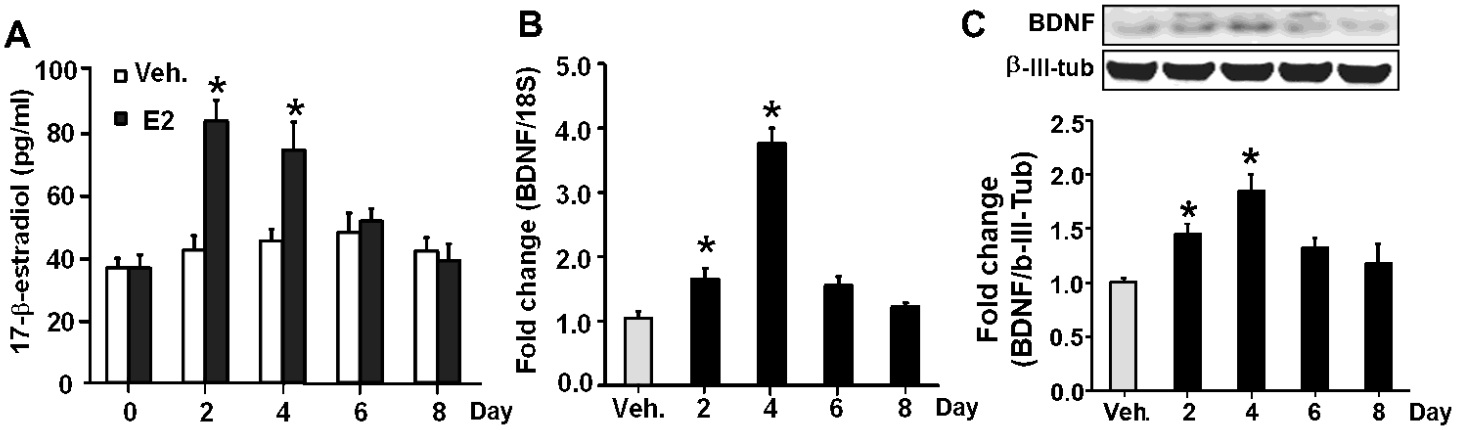

Figure 5

BDNF expression in lumbar-sacral spinal cord is regulated by estrogen. A. Plasma estrogen levels in cycling females that received a bolus estradiol (E2) infusion on day 1 (n= 8 rats in each group, two-way ANOVA, *P<0.05 vs. vehicle group). B. Lumbar sacral spinal cord BDNF mRNA following bolus estrogen infusion. C. Lumbar sacral spinal cord BDNF protein following bolus estrogen infusion.

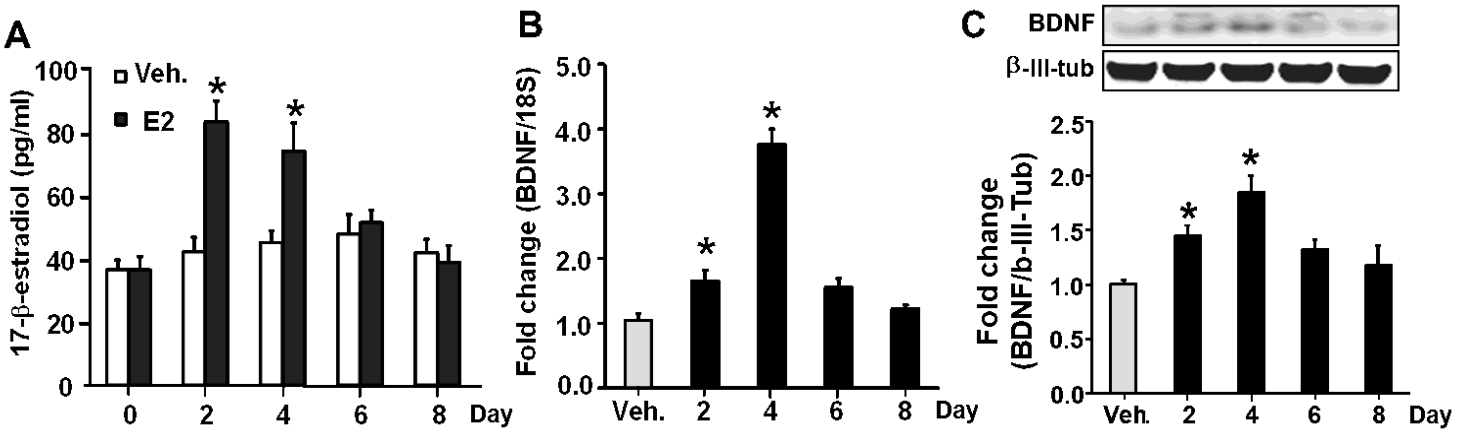

Figure 5

BDNF expression in lumbar-sacral spinal cord is regulated by estrogen. A. Plasma estrogen levels in cycling females that received a bolus estradiol (E2) infusion on day 1 (n= 8 rats in each group, two-way ANOVA, *P<0.05 vs. vehicle group). B. Lumbar sacral spinal cord BDNF mRNA following bolus estrogen infusion. C. Lumbar sacral spinal cord BDNF protein following bolus estrogen infusion.

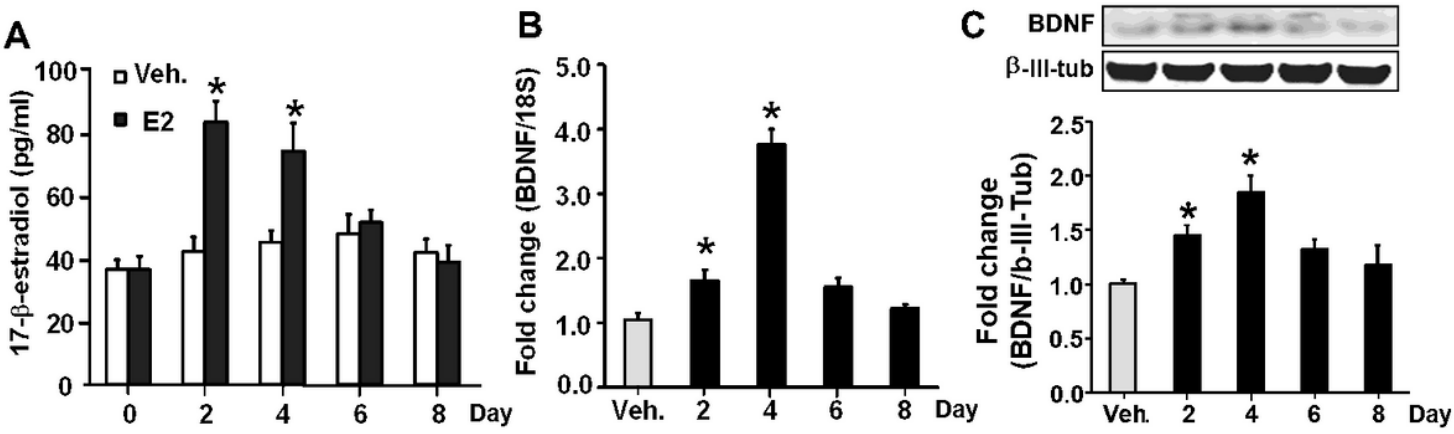

Figure 5

BDNF expression in lumbar-sacral spinal cord is regulated by estrogen. A. Plasma estrogen levels in cycling females that received a bolus estradiol (E2) infusion on day 1 (n= 8 rats in each group, two-way ANOVA, *P<0.05 vs. vehicle group). B. Lumbar sacral spinal cord BDNF mRNA following bolus estrogen infusion. C. Lumbar sacral spinal cord BDNF protein following bolus estrogen infusion.

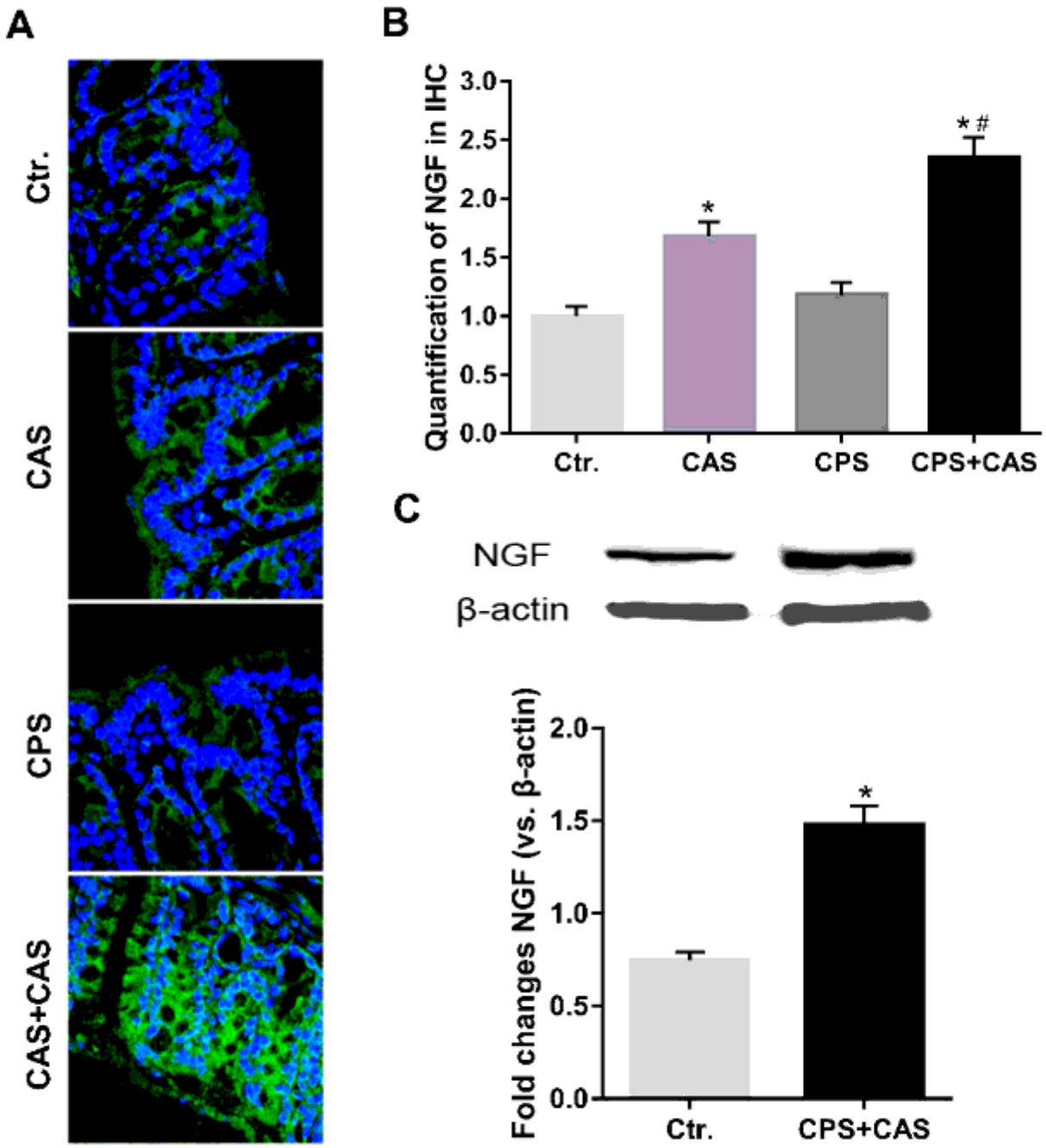

Figure 6

Nerve growth factor (NGF) expression level in colon wall. A. Immunohistochemistry of NGF (green) was detected with nucleus co-staining (blue) from control, CAS, CPS and CPS+ CAS group female rats' colon walls. 400x magnification representative pictures were shown. B. Quantification of NGF levels from colon wall in IHC (n=4 rats in each group, one-way ANOVA, *P<0.05 vs. control group, #P<0.05 vs. CPS group). C. Western blotting of NGF protein level from control and CPS+CAS female rats' colon wall tissue (n=6 rats in each group, t-test, *P<0.05 vs. control group).

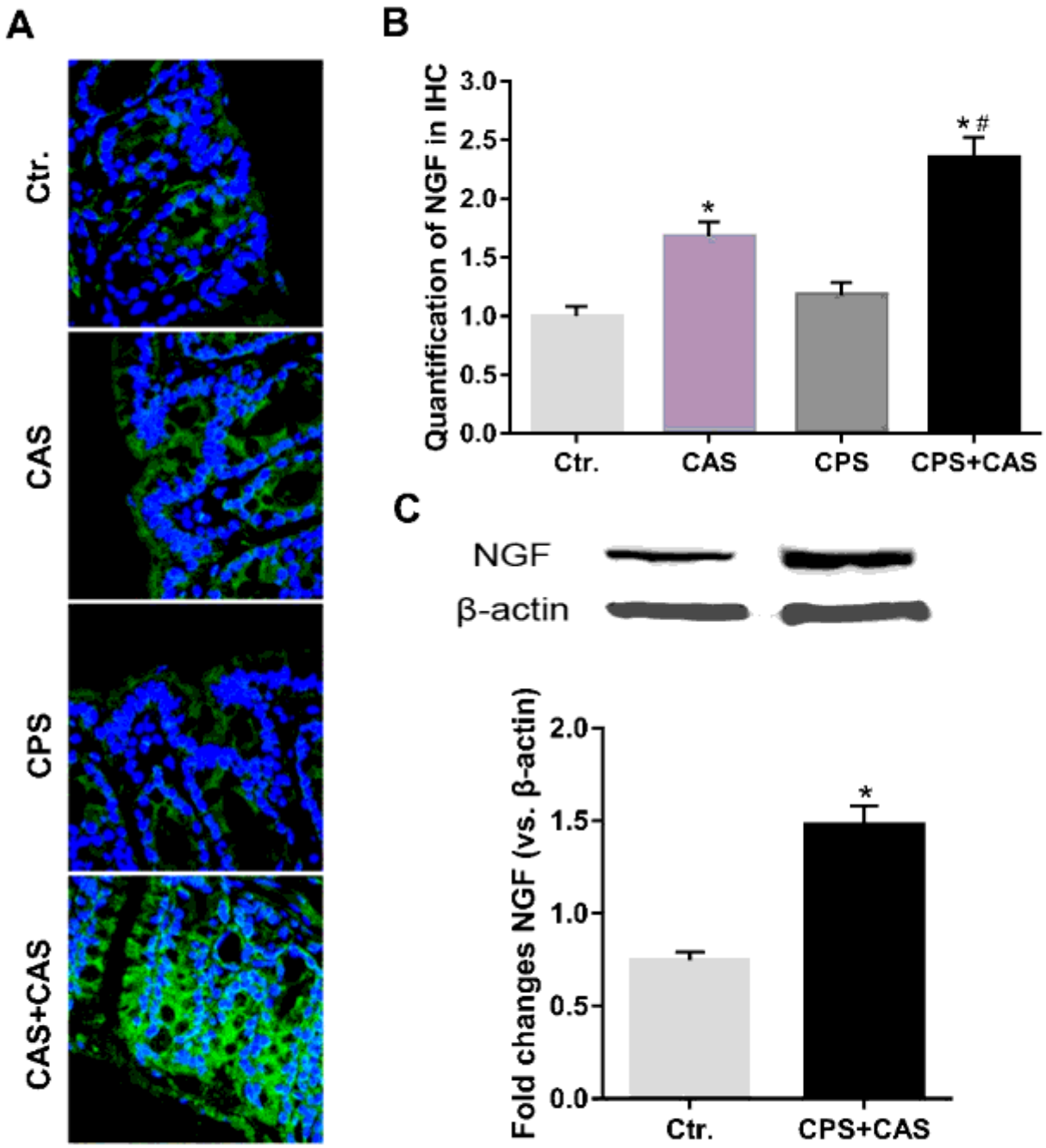

Figure 6

Nerve growth factor (NGF) expression level in colon wall. A. Immunohistochemistry of NGF (green) was detected with nucleus co-staining (blue) from control, CAS, CPS and CPS+ CAS group female rats' colon walls. 400x magnification representative pictures were shown. B. Quantification of NGF levels from colon wall in IHC (n=4 rats in each group, one-way ANOVA, *P<0.05 vs. control group, #P<0.05 vs. CPS group). C. Western blotting of NGF protein level from control and CPS+CAS female rats' colon wall tissue (n=6 rats in each group, t-test, *P<0.05 vs. control group).

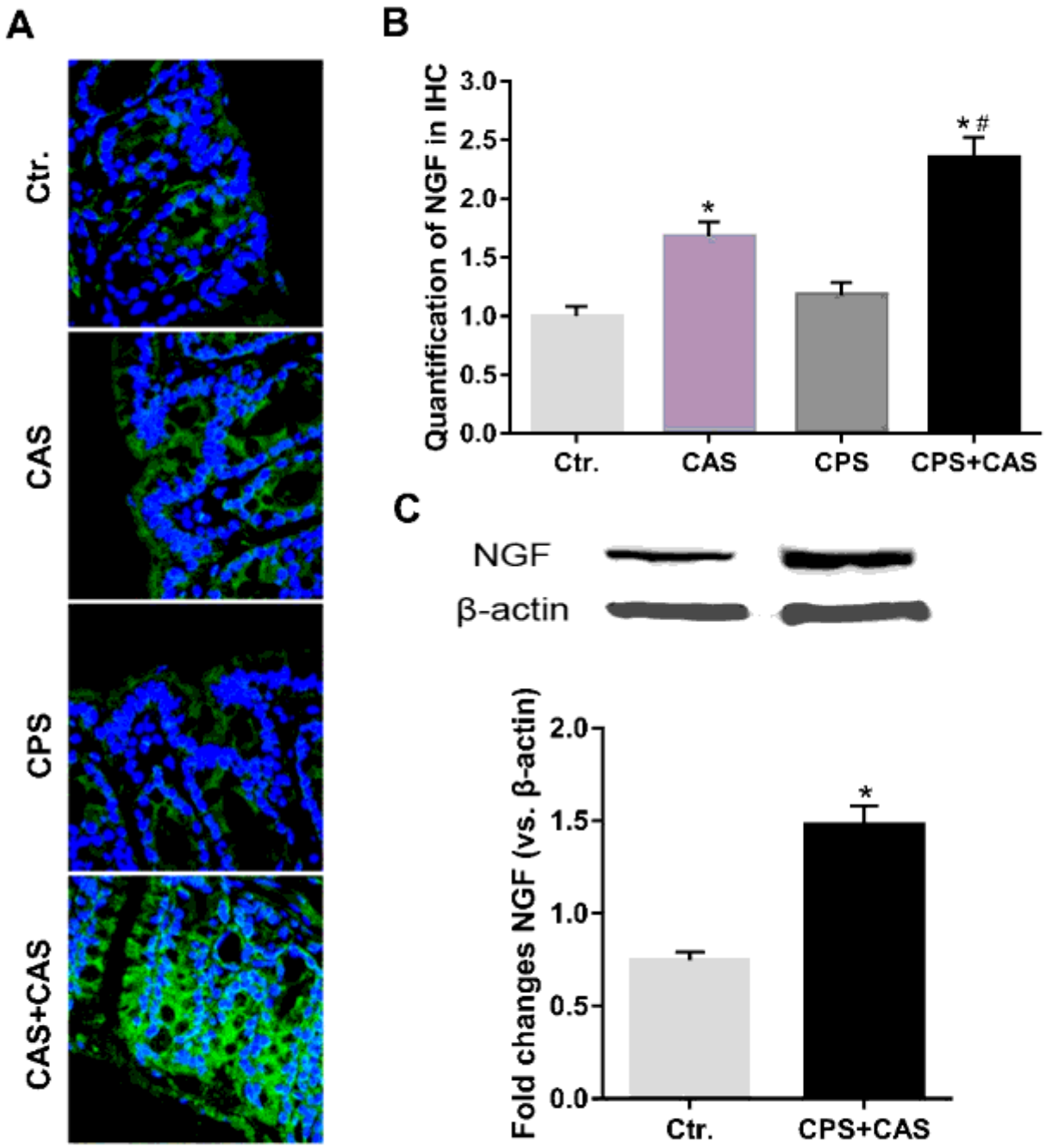

Figure 6

Nerve growth factor (NGF) expression level in colon wall. A. Immunohistochemistry of NGF (green) was detected with nucleus co-staining (blue) from control, CAS, CPS and CPS+ CAS group female rats' colon walls. 400x magnification representative pictures were shown. B. Quantification of NGF levels from colon wall in IHC (n=4 rats in each group, one-way ANOVA, *P<0.05 vs. control group, #P<0.05 vs. CPS group). C. Western blotting of NGF protein level from control and CPS+CAS female rats' colon wall tissue (n=6 rats in each group, t-test, *P<0.05 vs. control group).

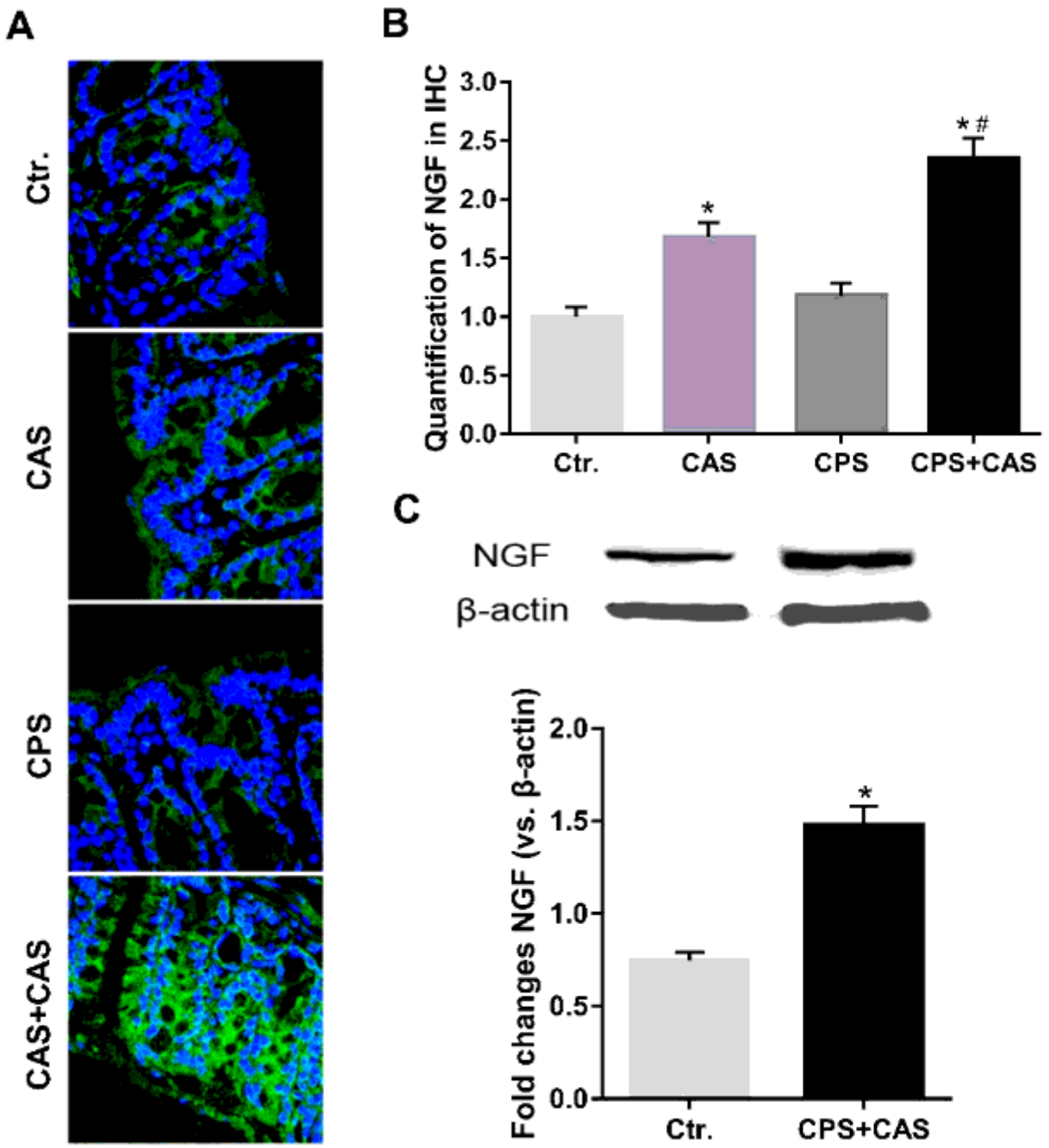

Figure 6

Nerve growth factor (NGF) expression level in colon wall. A. Immunohistochemistry of NGF (green) was detected with nucleus co-staining (blue) from control, CAS, CPS and CPS+ CAS group female rats' colon walls. 400x magnification representative pictures were shown. B. Quantification of NGF levels from colon wall in IHC (n=4 rats in each group, one-way ANOVA, *P<0.05 vs. control group, #P<0.05 vs. CPS group). C. Western blotting of NGF protein level from control and CPS+CAS female rats' colon wall tissue (n=6 rats in each group, t-test, *P<0.05 vs. control group).

Supplementary Files

This is a list of supplementary files associated with this preprint. Click to download.

- GraphicalAbstract.Png
- GraphicalAbstract.Png
- GraphicalAbstract.Png
- GraphicalAbstract.Png
- SupplementaryFigure.docx
- SupplementaryFigure.docx
- SupplementaryFigure.docx
- SupplementaryFigure.docx